DEPARTAMENTO DE CIÊNCIAS DA VIDA

FACULDADE DE CIÊNCIAS E TECNOLOGIA
UNIVERSIDADE DE COIMBRA

Role of Metformin as co-adjuvant in anticancer therapy targeting Osteosarcoma Cancer Stem Cells

Daniela Isabel Paiva de Oliveira

2013

DEPARTAMENTO DE CIÊNCIAS DA VIDA

FACULDADE DE CIÊNCIAS E TECNOLOGIA
UNIVERSIDADE DE COIMBRA

Role of Metformin as co-adjuvant in anticancer therapy targeting Osteosarcoma Cancer Stem Cells

Dissertação apresentada à Universidade de Coimbra para cumprimento dos requisitos necessários à obtenção do grau de Mestre em Bioquímica, realizada sob a orientação científica da Professora Doutora Célia Gomes (Universidade de Coimbra) e da Professora Doutora Carmen Alpoim (Universidade de Coimbra)

Daniela Isabel Paiva de Oliveira

2013

This work was developed in the following institution:

Pharmacology and Experimental Therapeutics, Institute for Biomedical Imaging and Life Sciences, Faculty of Medicine, University of Coimbra, Coimbra

A quem mais orgulho tem em mim

Agradecimentos

À Doutora Célia Gomes, orientadora deste projeto, os meus sinceros agradecimentos por todo o apoio, pelo incentivo, pela confiança e paciência demonstrados ao longo deste ano. Agradeço também por todo o conhecimento transmitido e por me "obrigar" a ser mais segura e crescer neste mundo.

À Professora Emília Duarte, coordenadora do Mestrado de Biologia Celular e Molecular, pelo apoio e interesse demonstrados durante os dois anos de mestrado.

Ao Doutor Antero Abrunhosa, do Instituto de Ciências Nucleares Aplicadas á Saúde da Universidade de Coimbra, pelo fornecimento de [^{18}F]FDG e pelo uso do equipamento adequado.

Ao Professor Doutor Carlos Alberto Fontes Ribeiro, dos Serviços de Farmacologia e Terapêutica Experimental, os meus agradecimentos pelo recebimento e instalações concebidas. E também a todo o *staff* deste serviço um muito obrigado pela simpatia sempre demonstrada.

À Magui por toda a alegria e ajuda prestada aqui e mesmo quando estava fora. À Cláudia um muito obrigado por todo o apoio, amizade, compreensão, companheirismo e ajuda dentro e fora do laboratório, um apoio muito importante ao longo deste ano.

Às companheiras da salinha, Tânia, Cláudia Amaral, Inês Pita, Sara e Catarina pelos cafés e pausas, pela hora de almoço, pela companhia e por tudo o que partilhámos.

Aos meus amigos e colegas Laura, Sérgio, Costa, Nando, Sónia, PP, Ruiva, Raquel, Catarina, Eli, Rui, Thony, Nádia, Tomás, Margarida por estarem presentes nestes 2 anos intensivos de Mestrado e por me ajudarem de uma maneira ou de outra.

Aos meus pais, irmãos e avós. Em especial á minha Mãe um sincero e sentido obrigado por tudo o que fez e faz por mim, por todos os sacrifícios, por me ouvir mesmo não sabendo o que se passa, por acreditar que sou capaz e não ter receio de arriscar em mim, por todo o amor, carinho e compreensão. Foi um enorme suporte este ano e sem ela eu nunca teria conseguido.

À minha Avó, quem adoraria poder oferecer-me a recompensa por esta etapa final e gritar aos sete ventos onde eu cheguei. A força que eu sabia que iria existir ajudou a ultrapassar vários momentos este ano e não poderei deixar cair isso em esquecimento.

Ao Ivo, por toda a paciência para conseguir aturar o meu mau-feitio e as minhas inseguranças, por ter sempre uma palavra de apoio e encorajamento, por estar sempre pronto para me amparar e ajudar no que eu precisasse. Obrigado pelo amor e paciência demonstrados nesta etapa importante da minha vida.

Index

List of Figures

List of Tables

List of Abbreviations

ABC	ATP-binding cassete
ALDH1	Aldehyde Dehydrogenase
AML	Acute Myeloid Leukemia
AMP	Adenosine Monophosphate
ATP	Adenosine Triphosphate
AMPK	AMP-activated protein kinase
Bak	Bcl-2 antagonist killer 1
BCA	Bicinchoninic Acid
Bcl-2	B-cell lymphoma protein 2
Bcl-X_L	Bcl-L related protein, long isoform
BCRP	Breast Cancer Resistance Protein
bFGF	basic Fibroblastic growth factor
BrDU	5-bromo-2'-deoxyuridine
BSA	Bovine serum albumin
$CCND_1$	Cyclin D1
CDK_4	Cyclin dependent kinase 4
CIS	Cisplatin
CSC	Cancer Stem Cell
CT	Computed Tomography
DHF	Dihydrofolate
DHFR	Dihydrofolate Reductase
DMEM/F12	Dulbecco's Modified Eagle Medium/ Nutrient Mixture F-12 Ham
DNA	Deoxyribonucleic Acid
DOX	Doxorubicin
DTT	Dithiotreitol
ECF	Enhanced Chemofluorescence Substrate
EDTA	Ethylenediaminetetraacetic Acid
E_2F	Elongation Factor 2
EGF	Epidermal growth factor
ELISA	Enzyme-Linked Immunosorbent Assay
EpCAM	Epithelial Cell Adhesion Molecule
ESC	Embryonic Stem Cell
EURAMOS-1	European and American Osteosarcoma Group Study
EZH_2	Enhancer of *Zeste Homologue* 2
FBS	Fetal bovine serum
[^{18}F]FDG	[^{18}F] fluoro-2-deoxyglucose
GLUT	Glucose transporter
IC_{50}	Concentration of drug necessary to inhibit cell proliferation by 50%
IFO	Ifosfamide
IGF	Insulin growth factor
IGFBP	Insulin growth factor binding protein
IGF1R	Insulin growth factor-I receptor
LKB1	Liver Kinase B1
MDM2	Murine double minute 2
METF	Metformin
MRI	Magnetic Resonance Imaging

MSC	Mesenchymal Stem Cell
mTOR	mammalian Target of Rapamycin
MTT	[3-(4,5-Dimethylthiazol-2-yl)-2,5-Diphenyltetrazolium Bromide]
MTX	Methotrexate
Oct4	Octamer-binding Transcription Factor 4
OS	Osteosarcoma
p53	p53 tumor suppressor protein
PCOS	Polycystic Ovarian Syndrome
PET	Positron Emission Tomography
PFA	Paraformaldehyde
Pgp	P-glycoprotein
pRB	Retinoblastoma Phosphoprotein
PVDF	Polyvinylidenedifluoride
RB	Retinoblastoma tumor suppressor gene
RPMI	Roswell Park Memorial Institute (Medium)
SD	Standard deviation
SDS	Sodium dodecyl sulphate
SEM	Standard error of mean
SFE	Sphere forming efficiency
Shh	Sonic-Hedgehog
SP	Side population
TGFβ	Transforming Growth Factor β
THF	Tetrahydrofolate
TIC	Tumor initiating cells
TP53	p53 tumor suppressor gene
TSC2	Tuberous Sclerosis protein 2
VER	Verapamil
WHO	World Health Organization

Abstract

Background: Osteosarcoma (OS) is the most common malignant primary bone tumor that appears in childhood and adolescence. It was recently demonstrated that OS possesses a small population with stem-like features, CSCs, which are responsible for the heterogeneity and regenerative ability of tumor cells and are considered responsible for the resistance to conventional therapies, namely chemotherapy and radiotherapy. Metformin (METF) is one of the most prescribed drugs to treat type II diabetes and in the past decade METF gained special attention in cancer treatment because of its anticancer properties. In this study we propose to explore the potential role of METF as an adjuvant of doxorubicin (DOX) to target CSCs from OS, exploring the effects and signaling pathways underlying the anticancer properties of metformin on OS CSCs.

Methods: CSCs were isolated from two human OS cell lines MNNG/HOS and MG-63 through the sphere–forming assay and then characterized regarding the expression of stem cell-specific transcription factors by immunofluorescence. The effects of MEFT on cell viability and proliferation was evaluated using the MTT and BrdU assays, respectively, and on sphere formation and self-renewal of CSCs. We also studied the chemosensitizing properties of METF on DOX cytotoxicity in both parental and corresponding CSCs. The metabolic state of cells following exposure to METF was assessed based on [^{18}F]FDG uptake. The phosphorylated form of AMPK, which is the main target of METF and of mTOR were analysed by Western blot.

Results: Both human OS cell lines MNNG/HOS and MG-63 contain sphere-forming cell subsets with stem-like properties expressing Oct4 and Nanog pluripotency markers, which are relatively more resistant to DOX than their differentiated counterparts. METF reduced the proliferation rate and viability of both cell types but was preferentially cytotoxic to CSCs relative to parental cells in a dose-dependent manner, and decreased the sphere-forming and self-renewal ability of both CSCs populations. Moreover, METF potentiate the cytotoxic effects of DOX in both cell populations, although the chemosensitizing effect has been more pronounced against CSCs. METF stimulates [^{18}F]FDG uptake in parental differentiated cells but not in CSCs. Exposure to METF induced dose-dependent increase in AMPK activation, with a more pronounced effect in CSCs.

Conclusion: MEFT demonstrated a preferential cytotoxicity against CSCs relatively to corresponding parental cells and inhibit the sphere-forming and self-renewal of CSCs. METF induce activation of AMPK and potentiates the cytotoxic effects of DOX mainly in CSCs. Collectively

our results suggest that METF combined with DOX may be an effective treatment strategy for targeting CSCs in OS.

Keywords: osteosarcoma; cancer stem cells; metformin; doxorubicin; co-adjuvant

Resumo

Introdução: Osteossarcoma (OS) representa o tumor ósseo primário mais comum aparecendo frequentemente na infância e adolescência. Recentemente foi demonstrada a presença de uma população com características de células estaminais em OS, as células estaminais cancerígenas (CSCs), que são consideradas responsáveis pela heterogeneidade e capacidade regenerativa das células tumorais. Para além disso, são também responsáveis pela resistência a terapias convencionais, como quimioterapia e radioterapia. Metformina (METF) é um dos fármacos mais prescritos no tratamento da diabetes tipo II. Na última década tem ganho especial atenção no tratamento contra o cancro devido às suas propriedades anticancerígenas. Neste estudo foi proposto explorar o papel da METF como adjuvante da doxorrubicina (DOX) tendo como alvo as CSCs de OS, para tal analisámos os efeitos e as vias de sinalização subjacentes às propriedades anticancerígenas da METF nestas CSCs.

Métodos: As CSCs foram isoladas a partir das linhas humanas de OS MNNG/HOS e MG-63 pelo método de formação de esferas e posteriormente caracterizadas tendo em conta a expressão de fatores de transcrição específicos de células estaminais, por imunofluorescência. Os efeitos da METF na viabilidade e proliferação celulares foi avaliada através dos ensaios de MTT e BrdU, respetivamente, e na formação de esferas e auto-renovação das CSCs. Também foi analisado o efeito "chemosensitizing" da METF na citotoxicidade da DOX em CSCs assim como em ambas as linhas parentais. O estado metabólico das células após tratamento com METF parentais foi permitido pela análise de captação de [^{18}F]FDG. A forma fosforilada de AMPK, que representa o principal alvo da METF e o mTOR foram analisados por *Western Blot*.

Resultados: Ambas as linhas celulares de OS MNNG/HOS e MG-63 contém uma subpopulação de células com características de células estaminais que expressam marcadores de pluripotência, Oct4 e Nanog. METF, as quais sais são relativamente mais resistentes à DOX do que as células parentais. A METF reduziu a taxa de proliferação e viabilidade em ambos os tipos celulares mas foi preferencialmente citotóxico para as CSCs, sendo este efeito dependente da dose. Também diminuiu a capacidade de formação de esferas e a sua capacidade de auto-renovação. Para além disso, a METF potenciou o efeito citotóxico da DOX em ambas as populações celulares, embora esse efeito tenha sido mais pronunciado nas CSCs. METF aumentou a captação de [^{18}F]FDG nas células parentais diferenciadas mas não nas CSCs. Exposição à METF induziu um aumento dependente da dose na ativação de AMPK, com um efeito mais pronunciado nas CSCs.

Conclusão: A METF demonstrou uma citotoxicidade preferencial para as CSCs relativamente às células parentais para além de que diminuiu a formação de esferas e a sua capacidade de auto-renovação. METF induziu a ativação de AMPK e potenciou os efeitos citotóxicos de DOX, principalmente nas CSCs. Em conjunto, os nossos resultados sugerem que o tratamento combinado de METF e DOX, pode ser uma abordagem eficaz na eliminação de CSCs no OS.

Palavras-Chave: Osteossarcoma; células estaminais cancerígenas; metformina; doxorrubicina; adjuvante

---

CHAPTER 1

INTRODUCTION

1.1. Osteosarcoma

1.1.1 Epidemiology

Osteosarcoma (OS) is the most common malignant primary bone tumor that appears in childhood and adolescence, comprising 20% of all bone tumors and 5% of pediatric tumors overall. It represents the sixth most common cause of cancer in > 15 years old children, and is considered an aggressive neoplasia. According to epidemiological studies in United States (US), it is a relatively rare bone tumor with approximately 400 new cases each year [1].

OS affects more males than females with a ratio of 1.6:1.The peak of incidence in females is earlier than in males due to the earlier onset of growth support. This disease appears frequently during puberty, where the growth support is highest, suggesting that the incidence of OS must be correlated with faster growing bone rate in puberty. Furthermore, several studies show that young OS patients at a growing age were taller than the normal population with the same age peak [2].

This tumor has a bimodal age distribution with a peak incidence of OS identified in young adults and the second peak of incidence identified in elderly adults. In the latter case, it is associated with Paget's disease of the bone, characterised by an abnormal bone remodelling, or as a consequence of treatment for a different cancer [3, 4].

OS was reported to occur in all bones of the body; however, it is most frequent in the lower long bones, arising at sites of rapid bone growth, such as distal femur (40%), proximal tibia (20%) and proximal humerus (10%). OS can also occur in axial skeleton, less than 10% of cases in the pediatric age group, most commonly in pelvis. OS grows radially forming a mass; when it penetrates the bone cortex it compresses the surrounding soft tissues. This pressure forms a pseudocapsular layer, which is referred to as "reactive zone", as we can see in Figure 1.1 [5, 7].

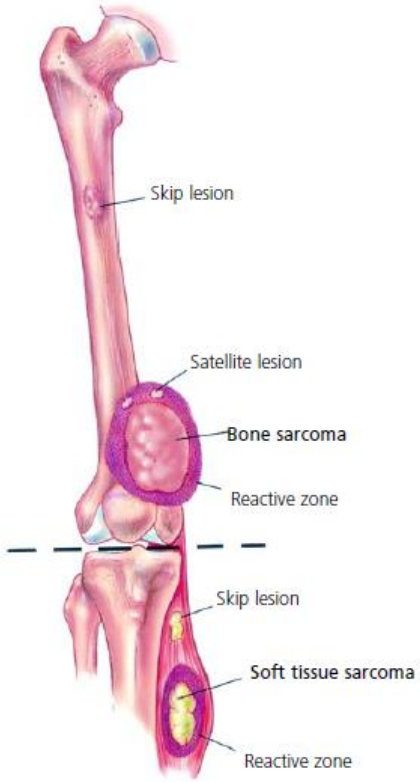

Figure 1.1. Osteosarcoma: Osteosarcoma grows radially forming a pseudocapsular layer consider as "reactive zone". Microscopic extensions can also appear and are referred to as satellite lesions. (Adapted from Wittig *et al.*, 2002)

1.1.2 Etiology

The etiology of this neoplasia is currently unknown; however, some genetic alterations have correlated with OS disease. OS is characterised by extensive and heterogeneous genetic complexity, which is reflected by the high level of genomic existing alterations [8].

Retinoblastoma tumor suppressor gene (RB1), located on chromosome 13, has a main role in the pathogenesis of OS. Genetic alterations in RB1 increase approximately 1000 times the incidence of OS. If a child has alterations in RB1, the most frequent second tumor is OS, increasing 500 times more the risk of developing OS when compared with healthy population.

Genetic analyses of tumor cells of OS show that 70% of the patients have homozygous loss of the RB gene and/or an alteration in RB gene production. The product of RB gene is a nuclear phosphoprotein (pRB) involved in the cell cycle control. During G1/S transition, it binds to E2F factors resulting in its activation and promotion of DNA synthesis and G1 to S transition [2, 9].

Furthermore, genetic alterations on p53 tumor suppressor gene (TP53) have also been related with OS occurrence. Activation of p53 gene induce cellular programmes including cell

cycle arrest, apoptosis or senescence that avoid accumulation of genetically altered cells. Moreover, p53 also play a role in angiogenesis, invasion and motility, glycolysis and autophagy. These findings suggest that p53 controls a variety of cellular genes network leading to the prevention of cancer development [8, 9]. Some studies show that OS appears spontaneously with high prevalence in mice which have heterozygous or homozygous mutation in the p53 gene. Also, the OS cell lines manifest p53 loss-of-function mutation that leads to lack of terminal differentiation of the osteogenic lineage. These findings support the hypothesis that OS occurs associated with a variety of mutations and a growth stimulus [11].

Also amplification and over-expression of murine double minute 2 (MDM2) and cyclin-dependent kinase (CDK4) have been seen in OS patients, suggesting that these genes are involved in OS pathogenesis. The MDM2 binds to p53 and sequesters it in the nucleolus, preventing the inactivation of p53 by the action of p14 protein; CDK4 gene product forms a complex with cyclin D1 (CCND1) which phosphorylates and inactivates the pRB, impairing the cell cycle regulation. Moreover, C-myc and C-fos proto-oncogenes are important in the regulation of cell growth and have been found to be amplified or over-expressed in OS cells. C-myc product is involved in regulating cell growth and DNA replication, and C-fos regulates genes involved in cell growth, differentiation, transformation and bone metabolism [2, 9].

In similarity with the previously mentioned genetic alterations the Wnt/β-catenin, Transforming Growth Factor- β (TGFβ), Sonic Hedgehog (Shh) and Delta-Notch signaling pathways, which are involved in cellular survival and proliferation, can appear unregulated in tumors, as in human OS [9, 12].

Other predisposing factors that could lead to the OS pathogenesis include exposure to ionizing radiation and Paget's disease. OS derived from exposure to ionizing radiation is rare and occurs after a long period of time and is mainly associated with a higher incidence of OS in adult [1].

1.1.3 Pathology and Origin of OS

The cell of origin of OS has been subject to intensive investigation but it is not completely clarified. The bone is a reservoir of growth factors and adult stem/progenitor cells and is also an organ with regeneration capacity. OS arises commonly near the growth plates of adolescents, the region with the most rapid skeletal growth, in which bone progenitor cells are actively in expansion, proliferation and differentiation. Hence, these cells have the support to develop malignant phenotypes [13].

Increasing evidence suggest that OS arise from mesenchymal stem cells (MSCs) or osteoprogenitor cells caused by genetic and/or epigenetic disruption that occurs during the osteoblast differentiation pathway, being characterized by the production of osteoid, an amorphous mineralized extracellular matrix lacking the characteristics of mature bone. Therefore OS has been regarded as a differentiation disease that results from any disruption occurring along the differentiation of MSCs into osteoblasts. MSCs are non-hematopoietic multipotent stem cells first discovered in adult bone marrow, although they can be found in adipose tissue and umbilical cord blood [9, 14]. These cells display self-renewal ability and multilineage differentiation potential along mesenchymal lineages including osteoblasts, chondroblasts and adypocytes, but also in cells of non-mesenchymal lineage (myocytes, cardiomyocytes, fibroblasts)(Figure 1.2) [4, 15].

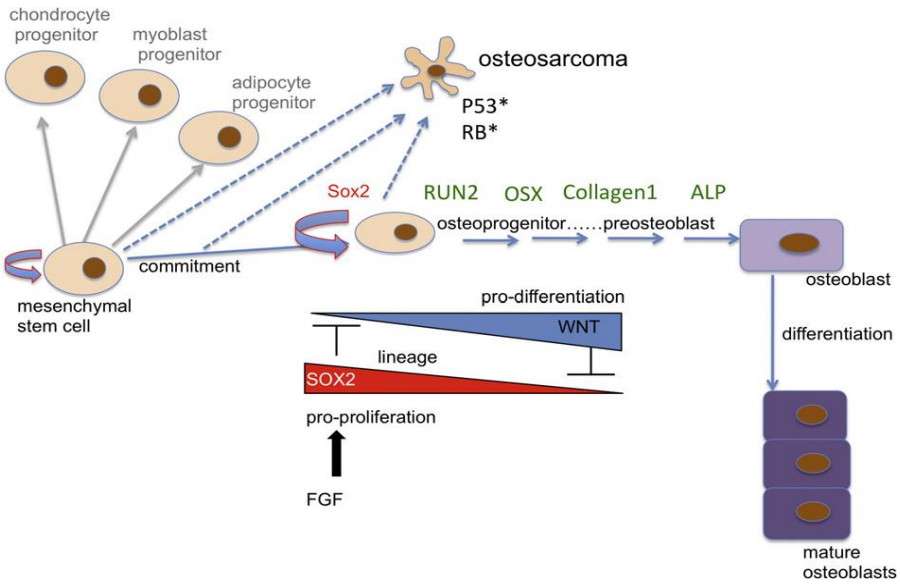

Figure 1.2. Differentiation of MSCs and progression of the osteoblastic lineage: MSCs can differentiate into nonhaematopoietic cell types, such as chondrocytes, myoblasts, adipocytes and osteoblasts. (Adapted from Basu-Roy *et al.*, 2012)

At diagnosis, 80% of OS is localized in one bone site and 20% of those cases have present lung metastasis. The lung is the most common site of metastasis, followed by bone. This type of pulmonary lesions are responsible for high mortality in OS patients.

The typical symptoms present in OS patients include pain and swelling that manifest after trauma or vigorous physical exercise. It appears later as a hard consistency mass and limitations in the join movement, also pathologic fractures may occur [2, 7, 24].

In order to confirm these symptoms radiological studies can be performed such as X-rays, magnetic resonance imaging (MRI) and computed tomography (CT) to study the extension of

the tumor and the involvement of surrounding structures (vessels, nerves, soft tissue); to check or determine the sites of metastatic disease and the intraosseous extent of the tumor can be performed a bone scintigraphy. The diagnosis is confirmed by histological examination of tumor obtained through an incisional or needle biopsy [2, 7]. Moreover, biochemical studies show an increase in alkaline phosphatase and also an increase in lactic dehydrogenase, these could be related with tumor volume and prognosis. Other prognostic indicators include extent of disease at diagnosis, size and location of the tumor, response to chemotherapy and surgical remission [9].

OS cells have similarities with osteoblast which are characterised as tumors that produce osteoid and can be classified in different subtypes of osteosarcoma depending on clinical, radiological and histological features [14, 17]. According to the World Health Organization (WHO), OS is histologically classified in three major subtypes: osteoblastic, the most common (70%), fibroblastic and chondroblastic (10% each), depending on the predominant type of matrix within the tumor (osteoid, fibrous or chondroid). Other less frequent types of OS are the telangiectatic, small cell, parosteal, periosteal, high-grade surface and secondary osteosarcoma [9, 24].

OS is considered a clinically and molecularly heterogeneous group of malignancies characterised by varying degrees of mesenchymal differentiation. In order to access this, we must underlie the alterations that occur in differentiation pathway and the stage of MSCs differentiation. Hence, studies of Cdnk2/p16 expression mRNA, which is the key regulator of MSC malignant transformation, can help us understand what can be affected in osteoblastic differentiation pathway. Loss of Cdkn2, in a later stage, is an important alteration which leads to MSC malignant transformation. This suggests that the MSCs give rise to osteogenic tumors after malignant transformation. Mohseny and collaborators (2009) confirmed this idea through *in vitro* and *in vivo* studies, where the loss of Cdkn2 locus is recurrent with consequent OS formation. Therefore, alterations in osteoblastic differentiation pathway cause production of osteoid (defective and immature) and/or bone tumor cells and there is highly proliferative malignant MSCs [9, 16]. Furthermore, it is believed that defects in the early stages of osteoblast differentiation pathway lead to the development of more aggressive and undifferentiated OS, as we can see in Figure 1.3 [9].

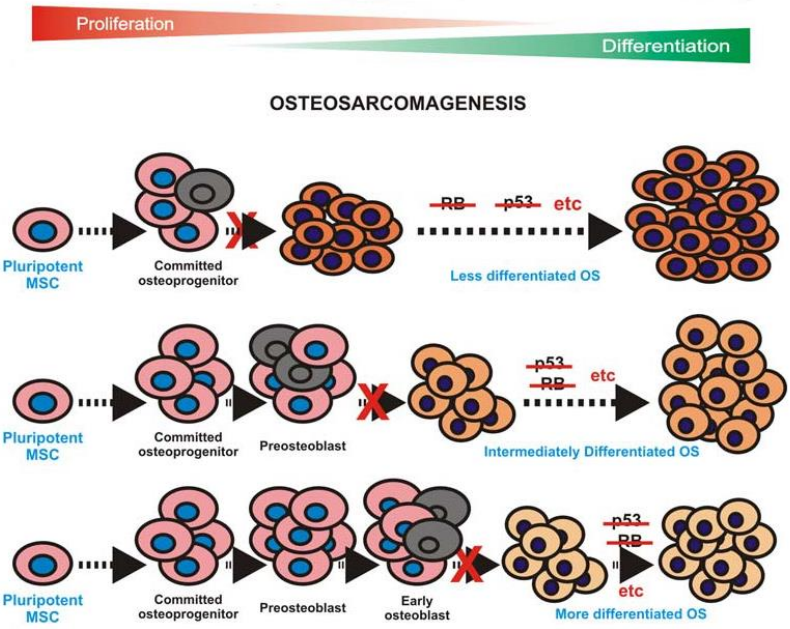

Figure 1.3. Osteosarcoma formation: Defects on osteogenic differentiation can lead to OS development. The genetic and epigenetic alterations can occur at different stages of osteogenic differentiation leading to the development of more aggressive and undifferentiated OS. (Adapted from Tang *et al.*, 2008)

1.1.4 Therapeutic approach

Before the 1970s the use of effective chemotherapy was not successfully established which lead to a poor outcome for patients with OS, with 2-year overall survival rates of 15%-20% following surgical resection and/or radiotherapy. 80% to 90% of those patients developed metastatic recurrence.

Over the past three decades, the introduction of high-dose multiagent neoadjuvant chemotherapy followed by surgical resection and adjuvant chemotherapy lead to a significant improvement in survival rates to approximately 65%-75% in patients without clinical evidence of metastatic disease at diagnosis [6, 18, 19].

Non-metastatic OS treatment regimens include pre-operative and post-operative chemotherapy. The goal of pre-operative or neoadjuvant chemotherapy is the reduction of tumor burden and the eradication of micrometastasis. The histological response to pre-operative chemotherapy, based on the % of tumor necrosis (based on the Huvos grade) has proven to be a prognostic factor for the clinical outcome of OS patients. Patients that present >90% of tumor necrosis are considered good responders and have a good prognostic with reported 5-year survival rate of 65%-75%. On the other hand, patients with < 90% tumor necrosis following therapy are considered poor responders and have a worse prognostic [1, 20, 21]. Despite the great improvement in survival rates with the introduction of multimodal

therapy, 20%-40% of patients with non-metastatic OS at diagnosis still relapse and die, mostly related with the development of resistance to this current treatment [14, 22].

However, some studies showed that an intensification of chemotherapy regimens can lead to the improvement of histological response but did not translate into a survival benefit [20, 23].

Presently, accordingly with European and American Osteosarcoma Group Study (EURAMOS-1) the most common protocols of chemotherapy applied are the administration of Doxorubicin (DOX), Cisplatin (CIS) and a high-dose of Methotrexate (MTX) [2, 24, 25].

Doxorubicin (DOX), also known as Adriamycin®, is an anthracycline antibiotic with strong antitumor activity against a wide number of tumors including breast, ovary, lung, liver and stomach cancers, Hodgkin's lymphoma and others [7, 26].

DOX acts by binding to DNA-associated enzymes, it can intercalate the base pairs of the DNA's double helix. By its binding to topoisomerase I and II, a variety of cytotoxic effects occur in addition to antiproliferation, resulting in DNA damage. Thus, the main mechanism of action of DOX appears to be the poisoning of topoisomerase II that results in double-strand DNA breaks, resulting in apoptosis. Furthermore, it has been demonstrated that DOX also forms adducts with DNA and these lesions are more cytotoxic than those induced by topoisomerase II impairment. Adducts are formed at 5'-CG-3' sites in DNA where the DNA sugar group is covalently linked to N2-amino group of guanine. The apoptosis pathway is triggered when the attempt to repair the breaks in DNA fail and cellular growth is inhibited at phases G_1 and G_2. Moreover, DOX can intercalate itself into the DNA, with the inhibition of both DNA and RNA polymerase, ceasing DNA replication and RNA transcription [27, 28]. This anticancer drug has a limited application due to its potential cardiotoxicity that provokes cardiomyopathy. Furthermore, DOX also can cause indirect toxicity in the brain and some patients present liver injuries [26, 27].

CIS, has a central role in cancer chemotherapy, mainly in testicular cancer [29], but can also be used in many others cancers, such as ovarian, cervical, head and neck, non-small-cell lung cancer [30] and in OS [31].

The main action of CIS occurs when it is activated by aquation and subsequently covalently binds to DNA forming DNA adducts. These adducts cause distortions in DNA and are recognized by several cellular proteins interfering with several signal-transduction pathways that provoke apoptotic cell death. Adducts formed by CIS and DNA can also avoid replication and transcription leading to the denaturation of DNA double helix [7, 30]. CIS also presents

several side effects, such as nephrotoxicity, peripheral neuropathy and ototoxicity, limiting the application of this anticancer agent [7, 18, 29].

MTX is another chemotherapeutic agent widely used in the treatment of several malignancies, namely breast, head and neck, bladder cancers, OS and non-Hodgkin lymphoma [33, 34]. MTX is an antifolate that blocks the folate-dependent enzyme dihydrofolate reductase (DHFR). This enzyme catalyses the conversion of dihydrofolate (DHF) to tetrahydrofolate (THF). DHFR is necessary for maintaining the intracellular pool of THF and its derivatives are essential cofactors in one-carbon metabolism. Furthermore, DHFR is pivotal in providing purines, pyrimidine and thymidines precursors for the biosynthesis of DNA, RNA and amino acids. Inhibition of DHFR through MTX reduces the folate pools necessary for the formation of purine and thymidine leading to the disruption of DNA replication [35]. Likely other chemotherapeutic agents MTX has secondary effects, provoking mainly renal failure accompanied by gastrointestinal, hematological and hepatic dysfunction [7, 33].

Ifosfamide (IFO) can also be applied in the treatment of OS [31]. This agent causes cross-linking of DNA strands, inhibiting the synthesis of DNA and proteins. This drug also presents toxicity leading to haemorrhagic cystitis and renal failure [7]. However, the combination of IFO and the chemotherapeutic agents used does not lead to an improvement in the survival rate [31].

1.2 The Cancer Stem Cell Hypothesis

OS, like other bone sarcomas is characterised by marked clinical, histological and molecular heterogeneity [36]. A significant functional and morphological heterogeneity can also exist within tumor cells comprising the tumor with significant implications in response to therapy [37]. Several factors can contribute to this phenotypic and functional heterogeneity, including genetic mutations, epigenetic changes, interactions between the tumor and the microenvironment [38].

Two models have been proposed to explain the tumor heterogeneity: the clonal evolution or stochastic model and the cancer stem cell (CSC) model. The clonal evolution model postulates that mutant tumor cells with growth advantages are selected and expanded and that all cells within this dominant population have equal capacity to regenerate the tumor. Furthermore, clonal evolution also provides the basis to understand the genetic mechanism of therapy resistance that can be acquired by cancer cells [37, 39]. During the last few years, the phenotypic and functional heterogeneity characteristics of solid tumors have been

subject of intense research and the CSCs theory emerged as a model to establish the heterogeneity and regenerative ability of tumor cells.

Accordingly to the CSCs hypothesis, tumors are hierarchically organized, such that only a small subset of cells with stem-like properties, which represents a reservoir of self-sustaining cells with the ability to self-renew, is responsible for sustaining tumorigenesis and establishing the cellular heterogeneity inherent in the primary tumor. These self-sustaining cells reside at the apex of the developmental pathway and were named as cancer stem cells, sharing some characteristics with normal stem cells [40, 41]. These two models are represented in Figure 1.4.

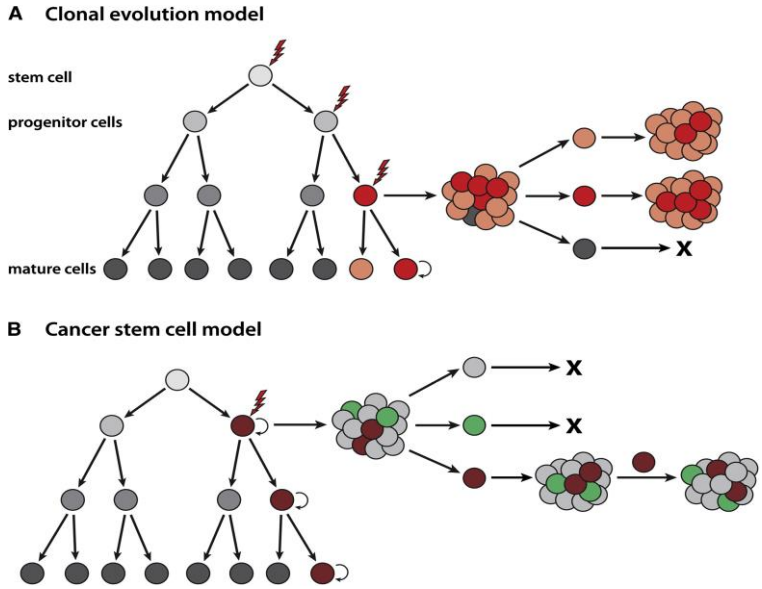

Figure 1.4. Tumor Heterogeneity Models: (A) In the nonhierarchical model mutations arising in tumor cells can confer to them a selective growth advantage. (B) Accordingly to the CSC model, tumors are hierarchically organized and sustained by a subset of cells with stem cell properties. These cells have the ability to generate heterogeneity through differentiation and maintain the tumorigenesis by self-renewal. (Adapted from Visvader *et al.*, 2012)

The CSCs have three distinct properties: the selective capacity to initiate tumors and drive neoplastic proliferation; the ability to create unlimited copies of themselves by self-renewal, and the potential to form mature non-stem cell cancer progeny by differentiation process [37, 38, 42]. These cells can divide asymmetrically leading to the formation of an identical daughter cell and a more differentiated cell, which, on subsequent divisions, creates the majority of tumor bulk, as described in Figure 1.5. The exact origin of CSCs is not completely clarified. It is hypothesized that these CSCs may arise through malignant transformation in normal stem cells or progenitor cells or in differentiated cells. Once these stem cells are more

susceptible to accumulate genetic mutations due to their long life span when compared to more differentiated cells, this is postulated. Furthermore, mutations can occur in differentiated cells that acquire the properties of stem cells and developed the capacity to undergo self-renew [42-44].

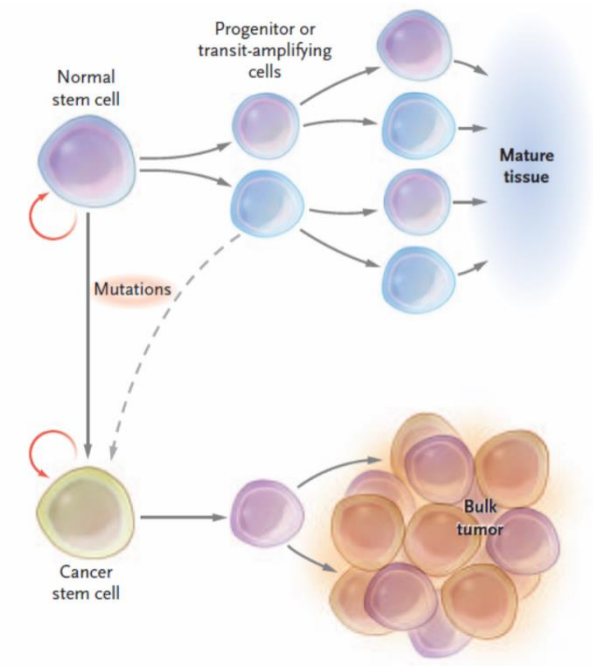

Figure 1.5. Cancer stem cells: Cancer stem cells can arise by mutations in normal stem cells or in progenitor cells, and subsequently undergo several divisions and differentiate to create primary tumor bulk. (Adapted from Jordan *et al.*, 2007)

1.2.1 Methods of identification of CSCs

The first evidence of the existence of CSCs subpopulation in tumors, also termed tumor-initiating cells (TIC), arise from studies on acute myeloid leukemia (AML) in 1994 [45]. Bonnet and Dick (1997) identified a small subset of cells with stem-like properties, based on the $CD34^{+}CD38^{-}$ cell surface phenotype, comprising 0.01-1% of the total population that induced leukemia, similarly to the primary tumor when transplanted into immunodeficient mice confirming their tumorigenic ability. The generation of leukaemia-like tumors was observed by serial transplantation into secondary immunodeficient mice, demonstrating the self-renewal potential of such cells and their ability to re-establish the phenotypic heterogeneity existing in the original tumor [45, 46].

Since then, CSCs have been isolated from several types of solid tumors, including breast, lung, colon, pancreas, liver, brain and OS [19, 47-52].

Several approaches, including functional assays and evaluation of immunophenotype have been explored to identify and isolate CSCs from both hematologic and solid tumors. However, any single method is capable of yielding a pure population of stem-like cells [42].

A panel of cell surface markers either singly or in combination have been used to identify CSCs in several tumors. This panel includes among others CD133, CD44, CD24, epithelial cell adhesion molecule (EpCAM), ATP-binding cassette B5 andABCG2. Nevertheless, even with a wide range of markers used to discern CSCs, none of these markers are exclusively expressed in CSCs of solid tumors, which emphasize the importance of establishing more specific markers, improving the knowledge of these markers for every tissue type [14, 54].

The CD133/AC133 (prominin-1) antigen is a pentaspan membrane glycoprotein, initially identified in neuroepithelial stem cells. CD133 was found to be expressed in cancer initiating cells in brain tumors, hepatocarcinoma, breast, pancreatic, lung and colon carcinomas and in OS and melanoma being considered a cancer stem cell marker. A population of $CD133^+$ cells in brain tumors, but not $CD133^-$, had the ability to grow under anchorage-independent conditions, formed tumors in immunocompromised mice, and exhibit stem-like features, such as differentiation ability, high proliferation rate and resistance to therapy [55, 56].

CD24 and CD44 have been proposed as markers for CSCs in several tumors. However, while some literature data referred to the existence of a population of cells with the $CD44^+/CD24^-$ phenotype and with stem cell characteristics in breast, prostate, colon, pancreatic and hepatic carcinoma, and also in melanoma [57], other literature data demonstrated that a subpopulation of $CD24^+$ cells could possess stem cell characteristics in colon and pancreatic tumors [58, 59], showed that the lack of CD24 is not an essential feature of CSC [56].

ABCG2 is a member of the ABC superfamily of transporters, which pump a variety of endogenous and exogenous compounds out of cells. It is recognized as a marker of stem cells and plays an important role in promoting stem cells proliferation and in the maintenance of its phenotype [60]. The overexpression of ABCG2 in CSCs is the molecular determinant for the identification of a side-population (SP) by flow cytometry based on the extrusion of certain dyes, such as Hoechst 33342 and Rhodamine 123 [61, 62]. Isolation of CSC through SP is a widely used method and supported by a variety of studies that revealed the presence of SP fraction in diverse human tumors, namely glioma [63], breast [64], ovarian and gastrointestinal cancers [65, 66]. Moreover, studies performed in our group, show the high expression of this drug efflux transporter and of P-glycoprotein (Pgp) other transmembrane transporter belonging to the ABC superfamily in human OS [67].

The identification of CSCs based on the ALDH1 expression was successfully applied to a hematopoietic stem cell population by Storms and collaborators (1999). These cells have high expression of ALDH1, a cytosolic enzyme that is responsible for oxidizing a variety of aldehydes into carboxylic acids; ALDH1 can also catalyse the conversion of vitamin A to retinoic acid, which is involved in stem cell differentiation [68, 69]. High levels of ALDH activity have been shown to characterize highly clonogenic, undifferentiated multipotential stem/progenitor cells and has been detected in many cancers including breast [70], liver [71], colon [72], AML [73] and OS [74] suggesting the presence of a subpopulation of cells with stem-like features.

Another functional method widely used to isolate CSCs is the sphere forming assay based on the ability of undifferentiated cells to form spherical colonies when cultured in serum-free medium under anchorage-independent conditions. Under these stressful growth conditions of anchorage independence and serum starvation, only undifferentiated cells can proliferate growing as spherical colonies in suspension, whereas differentiated cells are unable to proliferate and died. These spherical colonies enriched in stem-like cells, can long-term self-renew by serially passages and differentiate along multiple lineages which are defining properties of CSC. This method firstly performed for neural stem cells isolation has been used successfully with minor modifications, in the isolation of CSCs derived from a variety of tumors, including breast, neuronal and also in bone tumors [37, 75].

Gibbs and collaborators (2005) were the first to demonstrate the existence of CSC in OS through the sphere forming assay. These authors observed the formation of spherical colonies designed as sarcospheres when cultured in serum-free methylcellulose-based medium in the presence of growth factors and under non-adherent conditions. The sarcospheres expressed pluripotency markers characteristic of embryonic stem cells, further supporting the hypothesis that bone tumors contain cells with attributes of stem cells that can be isolated using the sphere-forming assay [36].

Studies performed by Martins-Neves *et al.*, in our laboratory, using identical methodology with few alterations, demonstrated the presence of sarcospheres in another OS cell line – MNNG/HOS. Those cells, not only express pluripotency markers Oct4 and Nanog, but can also differentiate towards osteogenic, chrondrogenic and adipogenic lineages when cultured in specific differentiating conditions; which reveal their multipotency towards mesenchymal lineages, a MSC characteristic.

1.2.2 Therapeutic Implications of CSCs

The existence of CSCs in tumors has significant therapeutic implications, once these cells possess several characteristics that turn them more resistant to conventional therapy relatively to their more differentiated tumorigenic counterparts. Features comprising relative dormancy/slow cell cycle kinetics, efficient DNA repair mechanisms, expression of specific drug-detoxifying enzymes, over expression of multidrug resistance related membrane transporters, resistance to apoptosis and protection by a hypoxic niche environment, with high production of free-radical scavengers can provoke the resilience of CSCs in the tumor [76]. Despite the considerable cytotoxicity of conventional chemotherapeutic drugs, not all cells present in tumor bulk are chemosensitive preventing an efficient eradication of tumor cells that subsequently leads to recurrence in following treatment [77]. Increasing evidence point out CSCs as resistant to both conventional chemo and radiotherapy and responsible for the recurrences commonly observed in cancer patients. The studies of Martins-Neves *et al.*, identified a resistant phenotype to both chemo and radiotherapy in sarcospheres isolated from the MNNG/HOS OS cell line [19].

As mentioned above CSCs can acquire resistance to chemotherapy and radiotherapy through a range of mechanisms already described. CSCs are recognized for their capacity to enter in a quiescent non-dividing G_0-state, without losing their proliferative ability, which appears to be necessary for preserving the self-renewal ability of stem cells. This feature is a critical factor in the resistance of CSCs to chemotherapy, since conventional chemotherapeutic agents target preferentially cells with high proliferative activity. CSCs that survive chemotherapy re-enter the cell cycle and initiate a cell division process that re-initiates the tumor growth [77].

Another feature of these cells, which confers their resistance to chemotherapy, is the high expression of drug efflux transporters from the ABC gene family, including P-glycoprotein (Pgp) and breast cancer resistance protein (BCRP). These pumps allow normal stem cells to preserve their genome protecting them against chemical agents. Data obtained by Martins-Neves *et al.* studies demonstrate a significant high expression of Pgp and BCRP in CSCs derived from human OS cell line compared to parental cells, which could explain the higher resistance of CSCs to chemotherapeutic agents (DOX and MTX). The reversal of resistance to chemotherapy with a non-specific inhibitor of ABC transporters and a transport substrate of Pgp and BCRP pumps sustain the hypothesis that up-regulation of such transporters prevents the intracellular accumulation of chemotherapeutic agents at toxic levels resulting in resistance [19]. SP cells can be isolated from a variety of cancer cell lines namely breast,

hepatocellular, gastrointestinal and thyroid that have shown high expression of ABC transporters when compared to the non-SP cells [62].

Moreover, those CSCs possess highly activated DNA repair mechanisms and possibly enhanced efficiency on DNA damage response activity. This property turns these CSCs radioresistant since they have enhanced capacity to repair lethal damages and present decreased production of ROS potentially as a result of increased levels of free radical scavengers. Furthermore, this capacity restrains them from undergoing apoptosis even with higher doses of irradiation and drugs [19]. In glioma patients with $CD133^+$ stem cells, those cells conferred resistance to radiotherapy with a more efficient mechanism of DNA damage repair and underwent less apoptosis [80].

Activation of apoptotic programme has been shown to be responsible for chemo- and radiation induced cytotoxicity in tumor cells, whereas inactivation of apoptosis signaling pathways help CSCs to evade the cytotoxicity activity of most anticancer therapies [54].

Recent studies in our laboratory, demonstrated that CSCs isolated from an MNNG/HOS OS cell line display increased resistance to DOX-inducing apoptosis as compared with parental cells, due to defects in the apoptotic mitochondrial signaling pathway. Analysis of the expression levels of the pro-apoptotic and anti-apoptotic proteins following exposure to DOX showed a significant overexpression of the anti-apoptotic proteins Bcl-2 and Bcl-X_L simultaneously with a reduction of pro-apoptotic protein Bak in CSCs in relation to parental cells [82].

Similar results were observed by Liu and collaborators (2006) in glioma cells that found high levels of Bcl-2 and Bcl-X_L in $CD133^+$ cells as compared with the non-stem cell fraction $CD133^-$ cells, further supporting the hypothesis that alteration in apoptosis pathways contribute for chemotherapy resistance in CSCs [78, 83].

All these studies suggest that CSCs have molecular pathways that promote their survival which increase the urgency to develop new therapies targeting specifically CSCs and achieve their ablation from the tumor [78].

Despite the current treatment with chemotherapy could shrink the tumor bulk the CSCs remain unharmed and following treatment these CSCs can self-renew and reshape the bulk of tumor leading to tumor recurrence as depicted in Figure 1.6 (a). However, whether a CSC-targeted therapy is combined with conventional therapy, CSCs would be killed and the tumor bulk also shrunk. Post-therapy any remaining non-CSCs could divide but with limited proliferative capacity and cells capable to reform the tumor bulk would be eliminated, so tumor recurrence would not occur as demonstrated in Figure 1.6 (b) [14].

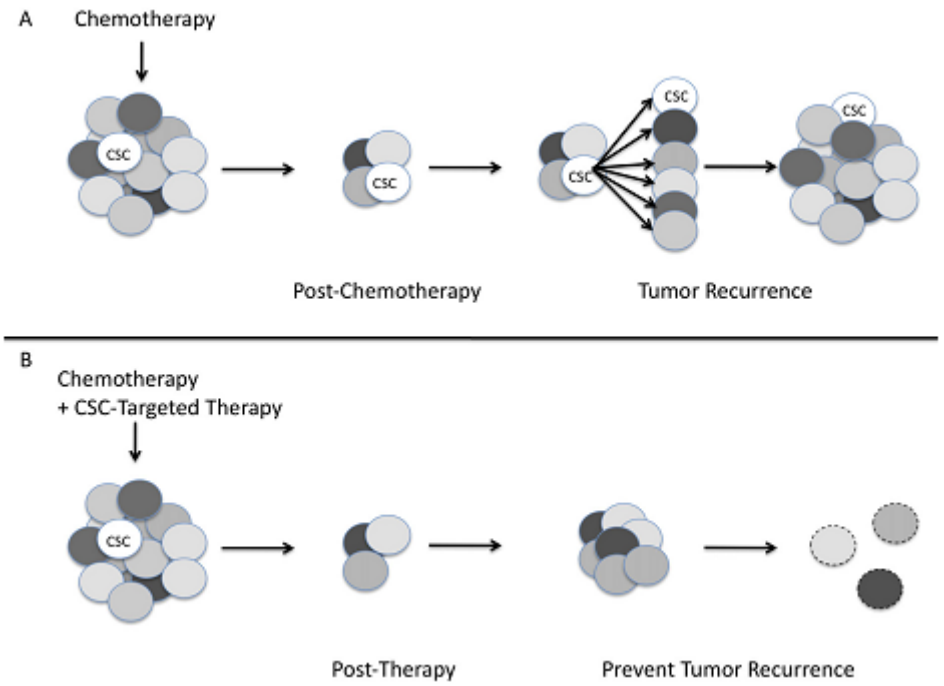

Figure 1.6. Impact of the CSCs model on anti-tumorigenic therapy. A) Chemotherapy alone shrinks the tumor bulk. However, CSCs that is chemoresistant might survive to this therapy and then can self-renew and differentiate in order to reform the tumor bulk. **B)** Combined chemotherapy will not only kill the tumor cells but also the CSCs. The remaining non-CSC tumor cells will die due to their limited proliferation capacity and the complete eradication of the tumor was achieved. (Adapted from Siclari *et al.*, 2010)

1.3 Metformin

Metformin (METF, 1, 1-dymethylbiguanide hydrochloride) is an insulin-sensitizing semi-synthetic biguanide with two methyl groups binding to the nitrogen nucleus as shown in Figure 1.7. This compound is derived from the hypoglycemic substance galegine and has potent antihyperglycemic properties [84].

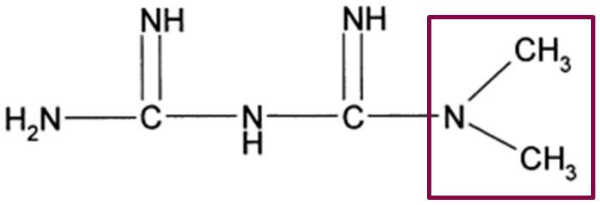

Figure 1.7.Chemical structure of Metformin. A semi-synthetic biguanide with two methyl groups binding to the nitrogen nucleus. (Adapted from Ruggiero-Lopez *et al.*, 1999)

METF is one of the most prescribed drugs to treat type II diabetes. This drug exerts its antidiabetic effects by decreasing hepatic glucose production and by increasing insulin sensitivity as well as glucose uptake and utilization by peripheral tissues [85]. The mechanism behind these actions is thought to be mediated by the inhibition of the mitochondrial oxidative phosphorylation leading to ATP/AMP imbalance, which results in the activation of AMP-activated protein kinase (AMPK), a central regulator of metabolic pathways. AMPK activation results in the inhibition of protein synthesis and gluconeogenesis during cellular stress.

Other indications of METF treatment include polycystic ovarian syndrome (PCOS), where insulin resistance is a key factor for development of metabolic disturbances, and the management of metabolic syndrome and diabetes prevention in high-risk populations [85].

In the past decade METF has gained special attention for its anticancer properties. Epidemiological studies have found that type 2 diabetic patients have an increased risk of developing liver, pancreatic, colorectal, endometrial, kidney, urinary, bladder and breast cancer. Insulin resistance and associated mitogenic hyperinsulinemia connect diabetes, obesity and metabolic syndrome with cancer. Numerous population-based epidemiological studies have found a lower incidence of cancer and lower mortality related with cancer in diabetic patients who have been treated with METF in comparison with patients that had been treated with other anti-diabetic drugs [84].

These epidemiological studies were performed in different tumor types including among others endometrial, colorectal or pancreatic carcinomas. More patients with colorectal and pancreatic carcinomas who had been treated with METF showed a 30% improvement in survival when compared with patients treated with other anti-diabetic agents [84, 89]. In addition, early epidemiological studies suggested an inverse relationship between diabetes and prostate cancer, presenting a 44% risk reduction of prostate cancer incidence in Caucasian men on METF therapy [84].

These findings from retrospective clinical studies suggest that METF may be associated with a decrease risk of developing cancer and with a better response to therapy, increasing the initial interest of METF as an anticancer agent. In fact, METF have received on last years, particular attention for its potential anti-tumorigenic effects that are thought to be independent of its hypoglycemic activity, and was recently suggested as an adjuvant treatment for cancer or gestational diabetes, and for the prevention in pre-diabetic populations.

Moreover, a retrospective study showed an increase in the effectiveness of neoadjuvant chemotherapy in breast cancer patients who took METF concomitantly with systemic therapy in patients with and without diabetes [84, 85].

1.3.1 Anti-cancer mechanisms of METF

The beneficial effects and potential mechanisms of METF in treatment of cancer have been attributed mainly to the activation of the AMPK/mTOR pathway under control of LKB1. LKB1 is serine-threonine acting as a tumor suppressor protein that is somatically inactivated in a variety of tumors. METF action in glucose metabolism is mediated through the activation of the tumor suppressor gene LKB1 in liver, as been suggested by Kourelis *et al*. Once activated LKB1 phosphorylates AMPK, which is inactive unless it is phosphorylated by upstream kinases in response to cellular metabolic stress. A direct consequence of the activation of AMPK is the inhibition of the mammalian target of rapamycin (mTOR), a downstream effector of growth factor signaling via tuberous sclerosis 2 protein (TSC2). mTOR is involved in regulating consuming cellular processes and plays a critical role in modulating cell growth and proliferation by controlling mRNA translation and ribosome biogenesis. The inhibition of mTOR decreases phosphorylation of S6 kinase, ribosomal protein S6 and eIF4E-binding protein 1, leading to cell cycle arrest and growth inhibition [85].

Cancer cells are more sensitive to nutrient starvation than non-malignant cells. Since AMPK is a major regulator of cell metabolism, it is activated by any condition that increases the ratio of AMP/ATP, leading to suppression of cellular metabolism and cellular proliferation. AMPK phosphorylates substrates which inhibit anabolic processes and induce catabolic processes to reverse the high AMP/ATP ratio. METF blocks the complex I of oxidative phosphorylation, which provokes an increase in NADH/NAD^+ ratio and blocks the fatty-acid β-oxidation and subsequent increase of AMP/ATP ratio. Due to this activation, AMPK inhibits protein synthesis by inhibition of both elongation factor-2 and mTOR pathway. AMPK phosphorylates TSC2 that form a tumor suppressor complex, TSC2-TSC1, and the TSC2

subunit inhibits Rheb GTPase activity leading to mTOR inhibition with a subsequent decrease in cell growth and proliferation. This METF's action may provide an explanation for its neoplastic actions. Furthermore, AMPK activation assists in adaptation to metabolic stress not only by cell growth and proliferation inhibition but also by inducing cell cycle arrest and/or apoptosis through p53 phosphorylation [85, 86, 92].

Activation of AMPK by METF has been shown in a variety of cancers, such as pancreas [91], breast [92], melanoma [93] and thyroid carcinoma [94].

Some studies performed in muscle tissue show that treatment with METF can induce a reduction in GLUT-1 content and this METF's action involves the subcellular redistribution of GLUT-1 in the skeletal muscle. However, METF treatment had no effect on the subcellular distribution of another transporter, the GLUT-4. Probably this is the main effect of METF to lowering the plasma glucose levels, however the main action is unknown [95]. Malignant cells have accelerated metabolism, high glucose requirements and increased glucose uptake. The increased glucose transport in malignant cells has been associated with increased and deregulated expression of glucose transporter (GLUT) proteins, with main characteristic features the overexpression of GLUT-1 and/or GLUT-3. Each of the GLUT proteins possesses different affinities for glucose and others hexoses. GLUT-1 and GLUT-3 have a high affinity for glucose, enabling a high rate of transport of glucose under physiological conditions. Since tumor has higher rates of glycolysis there is an increase activity of enzymes involved in glycolysis. Furthermore, upregulation of GLUT-1 and GLUT-3 expression occurs in the transformation process and could be a key role in the neoplastic process [96]. Furthermore, have been shown the presence of GLUT-1 and GLUT-3 in OS cell lines. In OS, insulin stimulates glucose transport due to increased GLUT-1 mRNA expression and increased expression of GLUT-1 protein [97]. So, METF could have an effect in cancer glucose uptake, which varies with tumor characteristics.

Other mechanisms include the induction of cell cycle arrest and apoptosis independently of AMPK activation. It was found that METF blocked cell cycle progression in G_0/G_1 phase in glioma cells and reduced levels of cyclin D1 in prostate cancer cells and blocked cell cycle in G_0/G_1 phase without AMPK activation. Furthermore, in pancreatic cancer cells METF was able to induce apoptosis by activation of the caspase pathway [85, 89].

In addition, increased levels of insulin growth factor 1 (IGF1) are associated with malignant transformation and tumorigenesis. Additionally, IGF1 has been shown to inhibit

chemotherapy-induced apoptosis by activation of the PI3K/Akt pathway. Since METF increases peripheral insulin sensitivity, thereby reverses hyperinsulinemia and inhibits the negative feedback of insulin on insulin growth factor binding protein (IGFBP1), IGF1 could be a useful target for METF's antineoplastic treatment. By applying METF therapy the reduction in insulin levels results in increased IGFBP1 levels. Consequently, IGF does not binds to its receptor and is not able to activate the PI3K/Akt/mTOR pathway, which plays a role in the control of protein synthesis and cell proliferation, leading to a decrease in tumor growth and proliferation [86]. Besides, Kourelis *et al.* (2012) demonstrated that METF did not activate AMPK in lung tissue but inhibited phosphorylation of insulin growth factor-I receptor (IGF1R), Akt and mTOR, supporting the hypothesis that METF could have other targets to achieve its anti-carcinogenic action [85]. The main actions of METF are depicted in Figure 1.9.

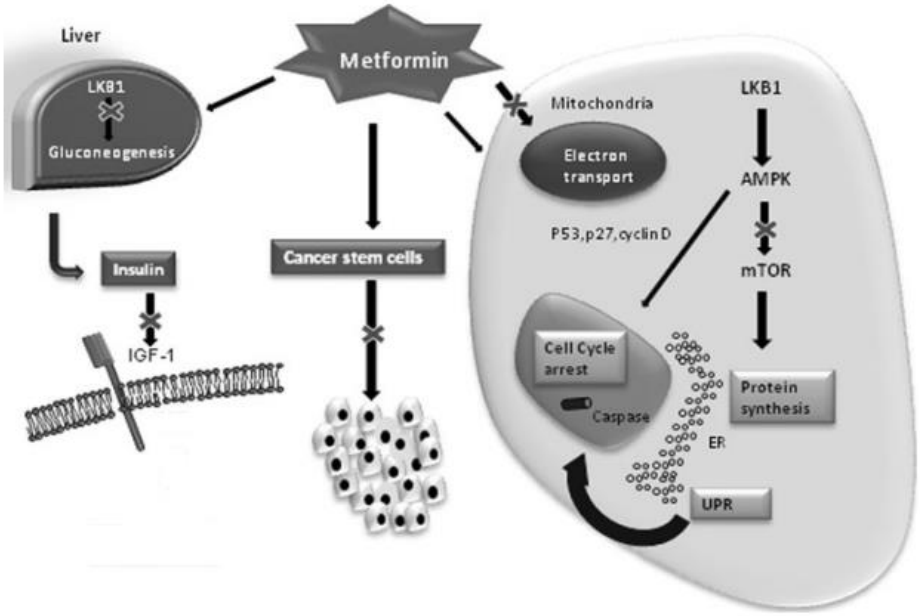

Figure 1.8. Possible mechanisms underlying METF inducing anticancer activity. Activation of AMPK by METF inhibits mTOR, induces cell cycle arrest and inhibits protein synthesis. METF could acts independently of AMPK through phosphorylation of cyclin D1 and p53, decreasing circulating insulin levels and exerting toxic effects on CSCs. (Adapted from Kourelis *et al.*, 2012)

Recent studies suggest that METF is preferentially toxic to CSCs. One of the proposed mechanisms of this effect in breast cancer is based on METF's ability to decrease systemic metabolic biomarkers such as insulin, IGF1 and estradiol, which are components of the mitogenic niches and regulators of the generation and/or maintenance of CSCs in their niche [84].

Bao and collaborators (2011) show that METF could specifically affect the formation of CSCs and their self-renewal ability from pancreatic cancer cells interfering with the expression of markers of CSCs, namely CD44 and EpCam, altering their genetic or epigenetic plasticity. Further in this study, the authors show that METF could decrease the gene expression of Enhancer of *Zeste Homologue 2* (EZH2) which is a histone methyltransferase involved in epigenetic regulation of gene transcription. Overexpression of EZH2 is related with *de novo* suppression of multiple genes in human cancers and might cause normal cells to dedifferentiate into stem cell-like by epigenetically repressing cell fate-regulating genes and tumor suppressor genes, which promotes the development of tumors. As well as EZH2, the expression levels of CD44, Oct4 and other pluripotency and stemness markers of CSCs were decreased after CSCs were treated with METF [88]. These studies suggest that treatment with

METF can decrease the capacity of sphere forming in breast and pancreatic cancer, an effect that was equally observed in lung and prostate cancers [88, 98, 100].

Moreover, METF have been implied in the Wnt/β-catenin signaling pathway regulation through AMPK activation. Unpublished data performed in our group, confirm the expression of β-catenin in CSCs derived from human OS cell lines. Since METF have been shown to attenuate Wnt/β-catenin signaling by reducing β-catenin protein levels in OS and also that β-catenin is expressed in CSCs from OS, can be suggested that METF acts on CSCs trough regulation of survival pathways [99]. Hirsch and collaborators (2009) show that the combination of METF with the chemotherapeutic agent DOX kills both CSCs and non-stem cancer cells populations in culture and also provokes a reduction in tumor growth and prolonged remission *in vivo* [99]. In addition, the combination of these two drugs increased the efficacy of therapy and diminished the side effects. Hence, an important effect of METF is decreasing the doses of conventional chemotherapeutic agents without decreasing their effectiveness, namely DOX [100].

Although typically the antitumorigenic effect of METF has been attributed to its ability to activate the LKB1/AMPK/mTOR pathway as well inhibition of insulin-growth mechanisms, the mechanism of action of this drug is complex and involve a multiple a variety of molecules and pathways with key roles in cell growth and survival [85].

1.4 Objectives

The main objective of this study was to explore the potential role of METF as adjuvant of DOX for targeting CSCs in OS. To achieve this goal we propose to:

✓ Isolate subpopulations of cancer stem cells (CSCs) in two human OS cells lines (MNNG/HOS and MG-63) using the sphere formation assay;

✓ Evaluate the effect of METF on cell viability, proliferation and metabolic activity;

✓ Evaluate the effect of METF on sphere formation and self-renewal abilities of CSCs;

✓ Evaluate the chemosensitizing effect of METF on cytotoxicity of DOX in parental cells and CSCs;

✓ Explore the signaling pathways underlying the anticancer properties of METF in OS CSCs.

CHAPTER 2

MATERIAL AND METHODS

2.1. Cell Culture

The human osteosarcoma cell lines MNNG/HOS and MG-63 was obtained from the *American Type Culture Collection* (ATCC, Rockville, MD). Cells were cultured in monolayer with RPMI-1640 medium (R4130, Sigma-Aldrich®, St. Louis, USA) supplemented with 10% (v/v) of heat-inactivated fetal bovine serum (FBS, 10270-106, Gibco® Invitrogen Life Technologies), 1% (v/v) antibiotic/antimicotic containing 100 mg/ml streptomycin, 100 units/ml penicillin and 0.25 µg/ml amphotericin (A5955, Sigma-Aldrich®, USA) at 37°C in a humidified atmosphere with 5% CO_2 and 95% air. Cells were subcultivated at a ratio of 1:5 twice a week when the cells reached approximately 80% of confluence. This procedure was made in sterile conditions in a laminar flow chamber.

2.1.1. Cell Counting and Viability

Cell counting and viability was determined before all experiments through the trypan blue exclusion method. For this procedure equal volumes of cell suspension and trypan blue 0.4% (Sigma-Aldrich®) (20µl) were mixed, transferred into a Neubauer chamber hemocytometer (Marienfeld, Germany) and then were observed and counted in an inverted microscope (Nikon, Eclipse TS 100). This experiment is based on the principle that viable and live cells with intact cell membranes can exclude the dye, while dead or injured cells with damaged membrane do not. In accordance with this, viable cells emerge brilliant with clear cytoplasm whereas nonviable cells appear blue. Cell viability was calculated as a percentage of viable cells relative to the total number of cells. Only cells exhibiting viability > 90% were used in all experiments.

2.2. Sphere Formation Assay

CSCs were isolated from MNNG/HOS and MG-63 parental cell lines through the sphere-formation assay in which cells were cultured in serum-free medium under anchorage-independent conditions as described elsewhere. [19] MNNG/HOS and MG-63 cells at a confluence of approximately 80% were detached with trypsin- ethylenediaminetetraacetic acid (EDTA) (T4049, Sigma-Aldrich®) and seeded at a density of 30×10^3 cells/mL in Petri culture dishes previously coated with 2.7 mg/cm^2 of Poly-HEMA (P3932, Sigma-Aldrich®) solution,

containing 13 mL of N2 medium with 1% methylcellulose (M0837, Sigma-Aldrich®). The N2 medium consists of Dulbecco's Modified Eagle Medium/Nutrient Mixture F-12 Ham (DMEM/F12, D2906, Sigma-Aldrich®) supplemented with 1.2 g/L sodium bicarbonate (S6297, Sigma-Aldrich®), 20 nM progesterone (P7556, Sigma-Aldrich®), 100 µM putrescine (P5780, Sigma-Aldrich®), 1% (v/v) insulin-transferrin-selenium-A supplement (Gibco® Invitrogen Life Technologies) and 1% (v/v) antibiotic/antimicotic. This medium was mixed with equal volume of sterile 2% methylcellulose solution to avoid the single-cell aggregation. Fresh aliquots of human epidermal growth factor 10 ng/mL (EGF, E9644, Sigma-Aldrich®) and of human basic fibroblast growth factor 10 ng/mL (bFGF, Prepotech EC, London, UK) were added twice a week. Cells were maintained at 37°C in a humidified atmosphere of 5% CO_2 and 95% air for 7-10 days.

After that, the spherical colonies formed were removed and transferred to adherent surfaces (T25 flasks, Orange Scientific, Belgium) and cultured in DMEM Low Glucose (Gibco® Invitrogen Life Technologies) medium supplemented with 10% of Mesenchymal Stem Cell-qualified serum (MSC), 2 mM Glutamine (59202C, Sigma-Aldrich®) and 1% (v/v) antibiotic/antimicotic. After reaching 70-80% confluence, cells were re-seeded as single-cell in serum-free medium and in non-adherent conditions for secondary sphere forming assay. This procedure was repeated three times for evaluating the self-renewal capacity of spheres. Second or third generation spheres were used in subsequent experiments and were termed as sarcospheres or CSCs.

2.3. Immunofluorescence assay

The expression and sub-cellular localization of the pluripotency transcription factors Oct4 and Nanog was analysed by immunofluorescence. Both parental (MNNG/HOS and MG-63) and corresponding CSCs were plated at a density of 150×10^3 and 130×10^3 cells/well, respectively, in 6-well plates covered with coverslips. After 48 hours the culture medium was removed and the cells washed with PBS (3 x 5min). After that the cells were fixed with 4% paraformaldehyde (PFA, P6148, Sigma-Aldrich®), during 10 minutes at room temperature and then washed with PBS (3 x 5min). After fixation cells were permeabilized during 10 minutes with 1% Triton-X at room temperature and subsequently washed with PBS (3 x 5 min) followed by incubation with blocking buffer (goat serum diluted in PBS/0.02% BSA) during 30 minutes in a humidified chamber. After blocking, cells were incubated with primary antibody diluted in PBS/0.02% BSA during 1 hour at room temperature, in a humidified chamber. The

primary antibody solution was removed and cells washed with PBS (3 x 5 min). After that cells were incubated with Alexa Fluor 594-labeled goat anti-rabbit IgG secondary antibody diluted in PBS/0.02% BSA during 1 hour at room temperature, in a humidified chamber protected from light. Afterwards, cells were washed with PBS (4 x 5 min) and incubated with 5 µg/mL Hoechst solution during 5 minutes for nuclei staining. Finally the cells were washed (3 x 5 min) in the dark, and the coverslips were mounted with Dako and sealed with nail polish. Images were captured on a confocal microscope (LSM 710 META, Carl Zeiss, Gottingen, Germany).

2.4. Cytotoxicity Studies to DOX and METF

Both parental MNNG/HOS and MG-63 cells and corresponding CSCs where assayed to their sensitivity to DOX, which is the most widely chemotherapeutic agent used in the treatment of OS, and METF as single agents or in combination. The cytotoxicity of DOX was analysed using the [3-(4, 5-Dimethylthiazol-2-yl)-2, 5-Diphenyltetrazolium Bromide] (MTT) colorimetric assay, a widely used method to assess cell viability. The effect of METF was analysed on cell viability using the MTT assay and on cell proliferation using the 5-bromo-2'-deoxyuridine (BrdU) incorporation assay. Since we intend to explore the synergy between METF and DOX on cell viability, the effects of the combined drugs was evaluated using the MTT assay.

Both parental MNNG/HOS and MG-63 and corresponding CSCs, previously expanded in adherent conditions and at 70% confluence, were detached with trypsin/EDTA, counted and seeded in 96-well plates (Sarstedt, Inc. Newton, USA) at a density of 7500 cells/well for MNNG/HOS and corresponding CSCs and 6000 cells/well for MG-63 and corresponding CSCs. Plates were maintained at 37°C overnight to allow the attachment of cells.

Next day, cells were incubated with different concentrations of drugs as a single dose and combined as described in Table 2.1.

Table 2.1 Drug concentrations and combinations used in cytotoxicity assays.

Single dose		Combined drugs	
DOX (µM)	**METF (mM)**	**DOX (µM) +**	**MET (mM)**
0.0001 0.01 0.10 0.25 0.50 1 5 10 50 100	0.05 0.1 1 2 5	0.25	0.05 0.1 1 2 5
		0.50	0.05 0.1 1 2 5
		1.0	0.05 0.1 1 2 5

Stock solution of DOX (DOXO-cell®, 2mg/mL) was diluted with PBS at appropriate working concentrations before adding to the cells. A stock solution of METF (Sigma-Aldrich) was prepared in PBS at a concentration of 1 mg/mL and was then filtered and diluted to yield the appropriate working concentrations.

2.4.1. Cell Viability Studies – MTT colorimetric Assay

Cell viability was determined using the MTT colorimetric assay. This experiment is based on the reduction of the yellow tetrazolium salt into purple formazan crystals by the mitochondrial enzyme succinate dehydrogenase of metabolic active cells, enabling the quantification of viable cells [102]. The amount of formazan crystals formed can be measured, after dissolution with acidified isopropanol, spectrophotometrically using an ELISA microplate reader. The colour intensity resulting from dissolution of formazan crystals is proportional to the enzyme activity and consequently to the number of viable cells.

Cell viability was determined after 48 h of treatment with DOX or METF as single doses and in combination as described in table 2.1. The culture medium was removed and 50 µL of MTT solution 0.5 mg/mL (M2128, Sigma-Aldrich®) were added to each well. The cells were further incubated at 37°C in the dark during 4 hours, the necessary time for the reduction of MTT with consequent formation of formazan crystals. Then, 50 µL of acidified isopropanol (0.04

M HCl) were added in order to dissolve the formazan crystals. The absorbance was read in an automatic ELISA microplate reader at 570nm with a reference filter of 620 nm.

The percentage of viable cells relatively to the controls was calculated using the following formula (1). Untreated or DOX-treated cells were used as controls for single-dose and drug combination studies, respectively.

$$\%\ Cellular\ Viability = \frac{Absorbance\ (Sample)}{Absorbance\ (Control)} \times 100 \quad (1)$$

The chemosensitivity of both parental and CSCs to DOX was estimated based on the calculation of the concentration of DOX needed to inhibit cell viability in 50% (IC_{50}). A dose-response curve was plotted on a semi-log scale with a percentage of viable cells *versus* concentration of DOX and fitted to a sigmoidal function, accordingly with the equation (2).

$$y = A1 + \frac{A1-A2}{1+10^{(LOG\ x_0-x)p}} \quad (2)$$

Where A1 and A2 are the bottom and top asymptotes, respectively, and x_0 is the IC_{50} and p the slope. The curve fitting was performed using GraphPad Prism software Version 5.0.

2.4.2. Cell Proliferation Studies – BrdU colorimetric Assay

The effects of METF on cell proliferation were evaluated using the 5-bromo-2'- deoxyuridine (BrdU) incorporation assay. BrdU is a synthetic nucleoside analogue of thymidine that is incorporated into the newly synthesized *DNA in proliferating cells*. The assay was carried out after the 48h incubation with METF using a commercial kit of Cell Proliferation ELISA, BrdU (Roche®, Germany) according to the manufacturer instructions. After cells treatment, the culture medium was removed and the cells were incubated with 100 µL of fresh medium containing 10 µL of BrdU solution (100 µM) at 37°C with 5% CO_2 during 3 hours. After that the medium containing BrdU was removed and the cells were incubated with 200 µL/well of fixative solution (*FixDenat*) during 30 minutes at room temperature to denature the DNA. Then, the fixative solution was removed and cells were incubated with 100 µL/well of anti-BrdU-POD solution, during 90 minutes at room temperature. Finally, cells were washed 3 times with 200 µL/well of washing solution and were incubated with 100 µL of substrate solution for 30 minutes at room temperature. The absorbance was read in an ELISA reader at 370 nm with a reference filter of 492 nm. Absorbance values were expressed as percentages relative to untreated controls.

2.4.3. Analysis of combined drugs effect

CompuSyn software was used to calculate the combination indices (CI) that indicate whether the effect of two drugs combination is higher than either alone, using the dose-response curves for each drug and the combination. CI values less than 0.85 indicate synergism, values equal to 0.90 indicates additivity and values greater than 1 indicates antagonism.

2.5. Cellular metabolic activity - [^{18}F]FDG uptake

The metabolic activity of both adherent OS cells (MNNG/HOS and MG-63) and corresponding CSCs was assessed using [^{18}F] fluoro-2-deoxyglucose ([^{18}F]FDG), which is a PET radiopharmaceutical analogue of glucose approved by Food and Drug Administration (United States of America) for routine clinical PET imaging studies.

Cells were seeded in 6-well plates at a density of 150×10^3 cells/well and allowed to attach overnight. Then, cells were incubated with increasing concentrations of METF (0.05-5 mM) during 48 hours. After this period, [^{18}F]FDG (0.75 MBq/mL) was added to the culture medium, and the cells were incubated for 1 hour in a humidified incubator at 37°C with 5% CO_2. Afterwards the culture medium was collected to glass tubes. The cells were washed twice with PBS, scraped and collected into glass tubes. Both tubes containing the collected culture medium and washing solutions or the scrapped cells were assayed for radioactivity in a Radioisotope Calibrator Well Counter (CRC-15W Capintec, USA) within the ^{18}F sensitivity energy window of 400-600 keV.

After reading radioactivity, cells were lysed with 1% SDS (m/v) in PBS (pH 7.0) and the total protein was quantified using the bicinchoninic acid (BCA, B9643, Sigma-Aldrich®) method with bovine serum albumin (BSA, A2153, Sigma-Aldrich®) as a standard in a 96-well cell culture plate that were used to generate a calibration curve. The reaction was incubated at 37ºC for 30 min. The absorbance was *read at 570nm* in an ELISA microplate reader. Results are reported as the percentage of cell radioactivity in relation to the total radioactivity added and were normalized per gram of protein. The cellular uptake of [^{18}F]FDG was expressed as a ratio to the levels found in METF treated cells to untreated cells.

2.6. Effects of METF on sphere-forming ability and self-renewal potential

To examine whether METF interferes with the sphere-formation ability of MNNG/HOS and MG-63 cells, we performed a sphere-forming assay as previously described in section 2.2 in the presence of METF at concentrations varying from 0.05 mM to 5 mM.

To further evaluate the effects of METF on the self-renewal of CSCs, which is a critical property of stem-like cells, first generation spherical colonies were enzymatically dissociated and platted in N2 serum-free medium containing METF (0.05 mM to 5 mM) in non-adherent surfaces to induce the formation of secondary spheres.

After 7-10 days in culture, the spherical colonies were observed and counted in an inverted microscope (Nikon, Eclipse TS 100). The sphere-forming efficiency (SFE) was calculated as the number of spheres formed divided by the original number of single cells seeded and expressed as the percentage. The sphere-size and morphological appearance was also evaluated. Images of the spherical colonies were acquired in a fluorescence microscope (Leica DFC350 FX, Leica Microsystems, Bannockburn, IL, EUA).

2.7. Analysis of Protein Expression by Western Blot

2.7.1. Expression of energy sensor AMPK and downwards targets

In order to explore whether exposure to METF induce the activation of AMPK, a major energy sensor in the cells, and lead to the inhibition of mTOR with consequent interference in protein synthesis and cell proliferation, we analysed the expression levels of the activated form of AMPK and mTOR in both parental and corresponding CSCs after 48h treatment with METF at different concentrations.

With this purpose, cells dissociated from sarcospheres and parental cell lines (MNNG/HOS and MG-63) were seeded in 6-well cell cultures plates (Orange Scientific, Belgium) in their corresponding culture medium at a density of 150×10^3 cells/well and allowed to attach overnight. Five increasing concentrations of METF ranging from 0.05mM to 5mM were added to each well. After 48 hours, the cellular extracts were prepared and the proteins analysed by Western Blot accordingly with the description in the section below.

2.7.1.1. Preparation of cellular extracts

The total extracts of MNNG/HOS and MG-63 and corresponding CSCs were prepared in the control situation and after 48h exposure to METF in the concentrations above mentioned.

Cells with a confluence of 70-80% were washed and scraped with PBS and then were centrifuged at 1400 rpm for 10 minutes. The cellular pellets were incubated with lysis buffer – RIPA [50mM Tris-HCl(pH 8.0), 150mM NaCl (Merck), 1% (v/v) Triton X-100, 0.5% (w/v) sodium deoxycholate, 0.1% (w/v) sodium dodecyl sulphate (SDS, 161-0307, Bio-Rad™) and 2mM EDTA], supplemented with a mixture of proteases and phosphatases inhibitors (Roche®), 2mM sodium orthovanadate, 1mM sodium fluoride (NaF) and 1mM dithiotreitol (DTT). After incubation for 30 minutes at 4°C in RIPA buffer, samples were sonicated dipped in ice in an ultrasound device (Vibra cell Sonics and Materials Inc. Danbury, CT USA) at 40 MHz, with 3-5 pulses for 5 seconds.

The protein concentration was quantified using the bicinchoninic acid (BCA, B9643, Sigma-Aldrich®) method with BSA (A2153, Sigma-Aldrich®) as a standard in a 96-well cell culture plate. This experiment is based on the formation of protein/Cu^{2+} complexes under alkaline conditions, followed by reduction of Cu^{2+} to Cu^{1+}. This reduction is proportional to the amount of protein present in the sample. Under alkaline conditions, the chelation of BCA with Cu^{1+} develop a blue/purple complex, which can be read in an automatic ELISA microplate reader at a wavelength of 562 nm [103].

The protein samples were mixed with an equal volume of 2x denaturing solution [0.25M Tris-HCl (pH 6.8), 200mM DTT, 20% (w/v) glycerol (G2025, Sigma-Aldrich®), 4% (w/v) SDS and 0.05% (w/v) bromophenol blue], and were heated at 95°C during 5 minutes for protein denaturation. The protein samples were stored frozen at -20°C until their use.

2.7.1.2. Sodium dodecyl sulphate polyacrylamide gel electrophoresis (SDS-PAGE) and electro-transference

Polyacrylamide gel preparation implies the crosslinking of acrylamide monomers used to support and separate the molecules based on size, shape or isoelectric point. The samples were loaded in SDS-polyacrylamide gels [7.5 or 12% of acrylamide (161-0148, Bio-Rad™)] and separated by electrophoresis during 90 minutes at 110V in buffer solution of 50mM Tris-HCl (pH 8.0-8.5) containing 50 mM bicine (B3876, Sigma-Aldrich®) and 0.1% (w/v) SDS. 60µg of the total extract protein from parental cells (MNNG/HOS and MG-63) and corresponding CSCs were used for immunoblot assay. A protein marker with known molecular weight – Precision PlusProtein™ Standards (161-0373, Bio-Rad™) was used in the electrophoresis.

After the electrophoresis, proteins were electro-transferred from the electrophoresis gel into hydrophobic polyvinylidenedifluoride membranes (PVDF,Millipore™, USA), previously activated in methanol (Merck, Germany). The electro-transference was performed in transfer

buffer [12.5mM Tris-HCl (pH 8.0-8.5) containing 96mM glycine (G8898, Sigma-Aldrich®) and 20% (v/v) methanol], applying a current of 110V during 90 minutes at 4°C.

2.7.1.3. Immunoblotting and Quantification

After transfer, membranes were blocked with 5% (w/v) non-fat dry milk in Tris-Buffered Solution (TBS: 20mM Tris, pH 7.6, 137mM NaCl) containing 0.1% (v/v) Tween20 (437082, VWR®)(TBS-T) during 1 hour at room temperature with soft agitation in order to reduce the non-specific protein interactions and to reduce the background signal. After that, the membranes were incubated overnight at 4°C with primary antibodies at appropriate dilutions, as shown in Table 2.2, in Phosphate Buffer Saline (PBS pH 7.4) containing 0.1% (v/v) Tween 20 (PBS-T), containing 5% (w/v) BSA or in TBS-T containing 1% (w/v) non-fat dry milk.

At the end of incubation period, membranes were washed 3 times for 10 minutes with PBS-T and then incubated with alkaline phosphatase-conjugated secondary antibodies (anti-mouse or anti-rabbit) for 1 hour at room temperature with agitation. Finally, membranes were washed again 3 times for 10 minutes with PBS-T and then revealed using the enhanced chemofluorescence substrate (ECF, Western blotting Reagent Pack, GE Lifesciences, Pittsburg, PA). The reactive bands were visualized on a Thyphoon FLA 9000 (GE Healthcare Bioscience, AB, Uppsala, Sweden) and were quantified using the ImajeJ software (Research Service Branch). The membranes were stripped using 0.2M NaOH for 5 minutes and then reprobed with anti-total-AMPK antibody in the case of pAMPK and with the anti-β-actin antibody as loading control, in the case of mTOR, followed by incubation with secondary antibody and revelation as described previously. The band intensities were normalized to their corresponding controls.

Table 2.2. Primary and secondary antibodies used on Western Blot, and corresponding dilutions.

Primary Antibody	Molecular Weight	Dilution	Company	Secondary Antibody	Dilution
pAMPK	62 kDa	1:1000	Cell Signaling Technology®	Anti-Rabbit	1:20000
AMPK	62 kDa	1:1000	Cell Signaling Technology®	Anti-Rabbit	1:20000
mTOR	289 kDa	1:2000	Millipore™	Anti-Rabbit	1:20000
β-Actin	43 kDa	1:10000	Millipore™	Anti-Mouse	1:20000

2.8. Statistical Analysis

All the results were presented as mean ± standard deviation (SD) or as mean ± standard error of mean (SEM), with *n* indicating the number of experiments performed. The Kruskal-Wallis non-parametric ANOVA test, with Dunnett's correction, was performed for multiple comparisons within the same cell line throughout different conditions. The Mann-Whitney non-parametric test was used to perform comparisons between two cell types under the same conditions. The statistical analysis was performed by using the GraphPad Prism software Version 5.0. The p-value < 0.05 was considered as statistically significant.

CHAPTER 3

RESULTS

3.1. Isolation and characterization of CSCs from MG-63 and MNNG/HOS cell lines

3.1.1. Isolation of sarcospheres from human OS cell lines

The presence of putative cells with stem-like properties in MNNG/HOS and MG-63 OS cell lines was identified through the sphere formation assay, in which parental cells were cultured in 1% methylcellulose serum-free medium, in anchorage-independent conditions. Under these conditions, both cell lines grew in suspension and formed spherical colonies, named sarcospheres as depicted in Figure 3.1. When transferred to adherent flasks and expanded in culture medium suitable for MSCs, cells started to migrate from the colonies and to adhere to the bottom of the flask. When re-seeded again in serum free-medium they formed secondary spherical colonies. This capacity to form spherical colonies was observed at least in a third round of sphere formation assay, which reveals the self-renewal ability of these cells which is considered an important characteristic of stem-like cells. Sarcospheres of second and third generation were used in succeeding studies and were termed as CSCs.

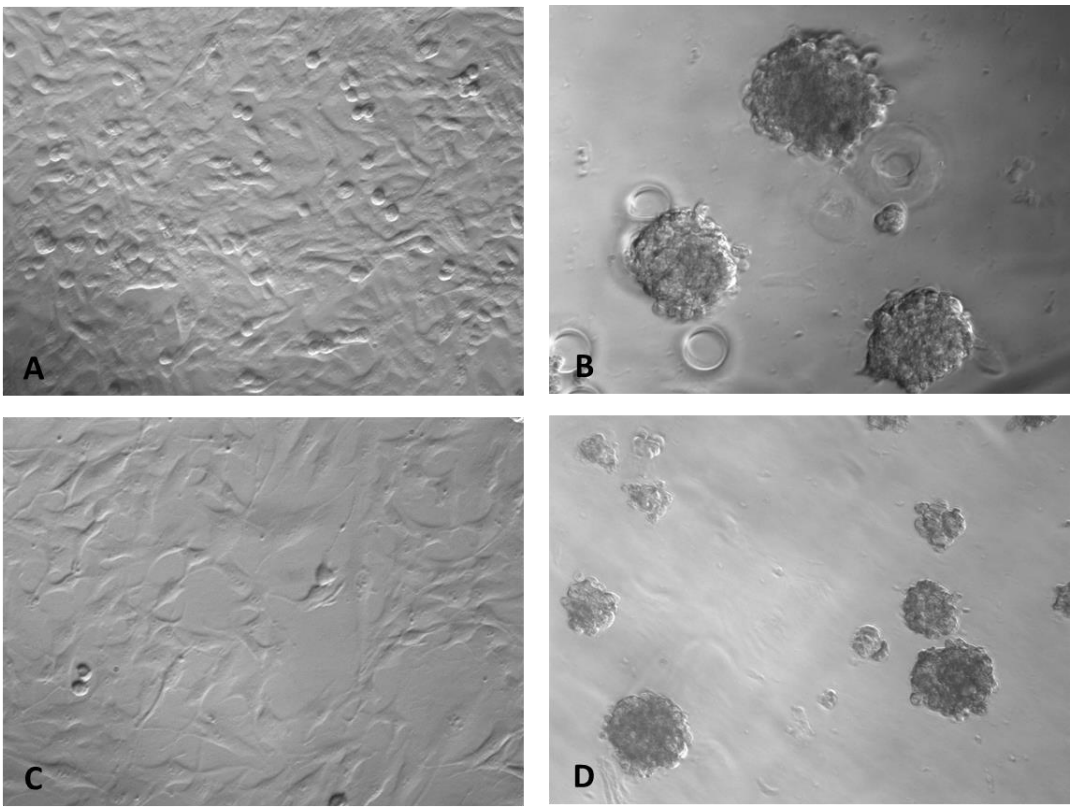

Figure 3.1. OS parental cell lines form sarcospheres in serum-free medium under anchorage-independent conditions. **A.** Adherent MNNG/HOS parental cell line. **B.** Sarcospheres isolated from MNNG/HOS cell line after 7 days in non-adherent conditions. **C.** Adherent MG-63 parental cell line. **D.** Sarcospheres isolated from MG-63 cell line after 7days in non-adherent conditions. (Original magnification: 200x)

3.1.2. Expression of pluripotency markers in human OS CSCs

Oct4 and Nanog are embryonic stem-cell specific transcription factors that play a role in the maintenance of self-renewal and pluripotency of stem cells and has been found to be up-regulated in CSCs. Confocal immunofluorescence analysis revealed the expression of Oct4 and Nanog in CSCs subpopulations localized both in the nuclei and the cytoplasm but none of the pluripotency-associated markers were detected in MNNG/HOS or MG-63 parental cells.

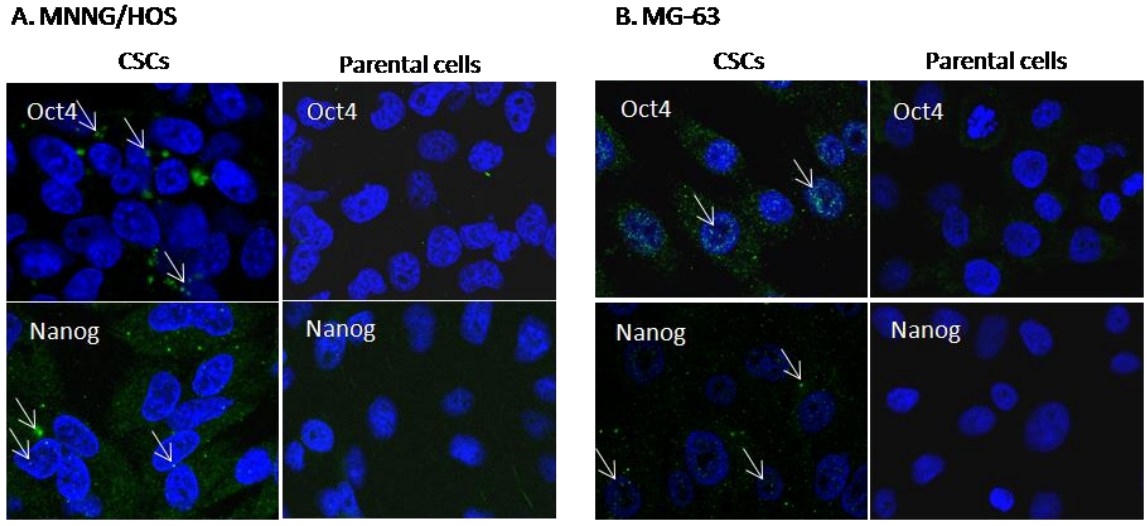

Figure 3.2. Representative confocal microscopy images of immunofluorescence staining for pluripotency markers Oct4 and Nanog in **(A)** MNNG/HOS and derived CSCs and **(B)** MG-63 and derived CSCs. Cells were counter-stained with Hoechst 33342 to identify cell nuclei. Arrows indicate the expression of Oct4 and Nanog in CSCs localized in the nuclei and in the cytoplasm. (Magnification 400x)

3.2. Effects of METF on cell viability and proliferation of OS cells

3.2.1. Effects of METF on cell viability of OS cells

Before starting the studies of co-administration of METF with DOX, we analyzed the effects of METF by itself in cells viability and proliferation, using the MTT and BrdU assays, respectively. This study was performed after 48h incubation with 0.05mM, 0.1mM, 1mM, 2mM and 5mM of METF.

METF induced a progressive decrease in cell viability of both MNNG/HOS and MG-63 parental cells and corresponding CSCs, although the effects are more pronounced for CSCs as depicted in Figure 3.3 and Table 3.1.

For concentrations above 1 mM (for MG-63 cells) or 2 mM (for MNNG/HOS cells) the percentage of viable CSCs is significantly lower ($p<0.05$) when compared with that in corresponding parental cells exposed to equal concentrations of METF.

The MG-63 cell line is less susceptible to METF-inducing cytotoxicity compared with MNNG/HOS cells. For MNNG/HOS cells, the reduction in cell viability was more pronounced (Figure 3.3 A, Table 3.1) and was significant for concentrations starting from 0.1mM, whereas for the MG-63 the effect on cell viability was inferior and only significant for concentrations above 1 mM (Figure 3.3 B, Table 3.1).

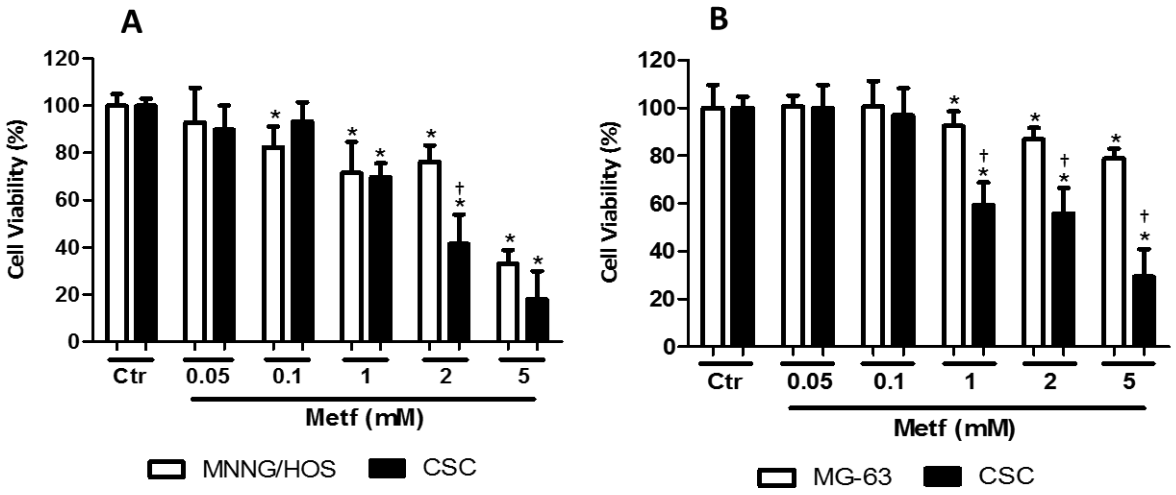

Figure 3.3. Percentage of viable cells after treatment with different concentrations of METF (0.05-5mM), for MNNG/HOS cells and CSCs (A) and MG-63 cells and CSCs (B). These results were presented as mean ± standard deviation (SD) from three independent assays (n=3) performed in triplicate.
*$p<0.05$ when compared with corresponding control cells (untreated)
†$p<0.05$ when compared with corresponding parental cell line, in the same conditions

Table 3.1. Effect of METF on cell viability of parental MNNG/HOS and MG-63 cells and corresponding CSCs.

	Cell Viability (%)			
METF (mM)	**MNNG/HOS**	**CSC**	**MG-63**	**CSC**
0	100.00 ± 5.03	100.00 ± 3.07	100.00 ± 9.64	100.00 ± 4.78
0.05	92.97 ± 14.64	89.95 ± 10.16	100.63 ± 4.64	100.07 ± 9.56
0.1	82.45 ± 8.83*	93.47 ± 8.11	100.63 ± 10.59	96.90 ± 11.31
1	71.60 ± 13.11*	69.88 ± 5.79*	92.42 ± 6.14*	59.37 ± 9.39*†
2	76.39 ± 6.90*	41.44 ± 12.48*†	86.97 ± 4.69*	55.82 ± 10.60*†
5	33.03 ± 5.80*	18.03 ± 11.89*	78.82 ± 4.11*	29.40 ± 11.59*†

Abbreviations: METF, metformin. Cells were incubated with increasing concentrations of METF (0.05-5mM) for 48 hours. Cytotoxicity was evaluated using the MTT colorimetric assay. Results are expressed as mean ± standard deviation (SD) of at least three independent experiments performed in triplicate.
*p<0.05 when compared with control cells (untreated)
†p<0.05 when compared with corresponding parental cell line, in the same conditions

3.2.2. Effects of METF on cell proliferation of OS cells

To investigate the effects of METF on cell proliferation we performed a BrdU incorporation assay. METF at low concentrations of 0.05 mM and 0.1 mM (within the range of the recommended therapeutic doses) did not reduced significantly cell proliferation neither of parental cells nor of corresponding CSCs populations, as depicted in Figure 3.4 and Table 3.2. Significant anti-proliferative effects of METF were observed for concentrations equal or above 1 mM in both parental and CSCs.

From the two CSCs populations, the one obtained from the MNNG/HOS cell line appears to be more susceptible to the anti-proliferative effect of METF, as indicated by the lower percentage of actively proliferative cells comparatively to MG-63-derived CSCs exposed to the same concentrations of METF (Figure 3.4 and Table 3.2).

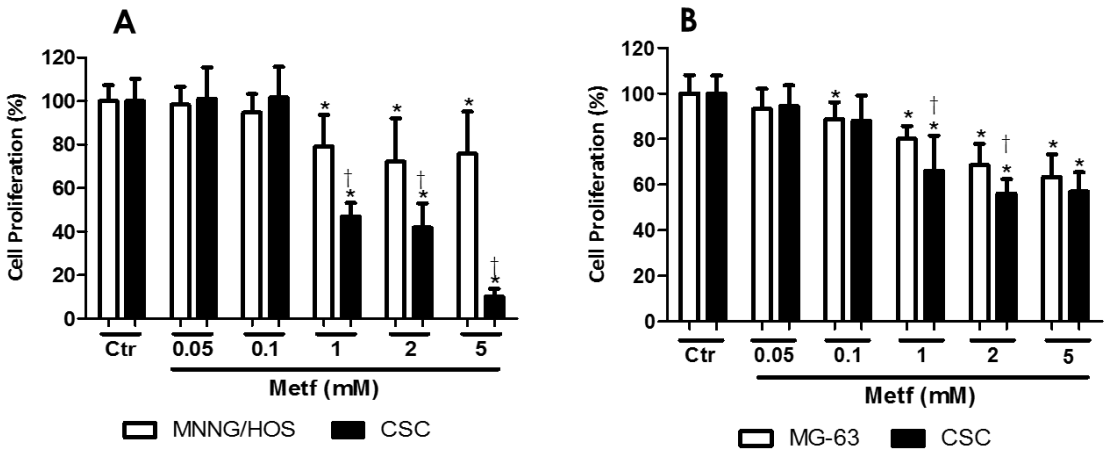

Figure 3.4. Percentage of proliferative cells after treatment with different concentrations of METF (0.05-5mM), for MNNG/HOS cell line and corresponding CSCs (A) and MG-63 cell line and corresponding CSCs (B). These results were presented as mean ± standard deviation (SD) from three independent assays (n=3) performed in triplicate for parental cell lines and in duplicate for CSCs.
*p<0.05 when compared with untreated parental cells
†p<0.05 when compared with corresponding parental cell line, in the same conditions

Table 3.2. Effect of METF on cell proliferation of parental MNNG/HOS and MG-63 cells and corresponding CSCs.

	Cell Proliferation (%)			
METF (mM)	**MNNG/HOS**	**CSC**	**MG-63**	**CSC**
0	100.00 ± 7.32	100.00 ± 10.23	100.00 ± 8.01	100.00 ± 7.82
0.05	98.34 ± 8.19	101.01 ± 14.43	93.25 ± 8.95	94.58 ± 8.92
0.1	94.72 ± 8.53	101.73 ± 14.02	88.70 ± 7.44*	88.02 ± 11.15
1	79.19 ± 14.48*	46.91 ± 6.29*†	80.09 ± 5.71*	66.06 ± 15.51*†
2	72.21 ± 19.80*	41.89 ± 11.08*†	68.53 ± 9.41*	56.14 ± 6.26*†
5	75.78 ± 19.36*	10.20 ± 3.55*†	63.38 ± 9.89*	56.90 ± 8.53*

Abbreviations: METF, metformin. Cells were incubated with increasing concentrations of METF (0.05-5mM) for 48 hours. Cytotoxicity was evaluated using the BrdU incorporation assay. Results are expressed as mean ± standard deviation (SD) of three (n=3) independent assays performed in triplicate for parental cells and in duplicate for CSCs.
*p<0.05 when compared with parental cell line (untreated)
†p<0.05 when compared with corresponding parental cell line, in the same conditions

3.3. Sensitivity of parental OS cell lines and CSCs to DOX

The cytotoxic effects of DOX, the main chemotherapeutic drug used in the treatment of OS, were evaluated in both parental MNNG/HOS and MG-63 cells and in corresponding CSCs. Cell

viability was assessed using the MTT colorimetric assay after 48h incubation with increasing concentrations of DOX (0.001-100µM).

The individual dose-response curves obtained and corresponding IC_{50} values are represented in Figure 3.5 and Table 3.3, respectively.

The treatment with DOX induced a decrease in cell viability in both parental MNNG/HOS and MG-63 cells and corresponding CSCs, in a dose-dependent manner. However, this effect was less marked for the CSCs compared to parental cells, as depicted in the dose-response curve of CSCs that is shifted to the right side; indicating that CSCs need a higher concentration of DOX to accomplish the same cytotoxic effect observed in corresponding parental cells.

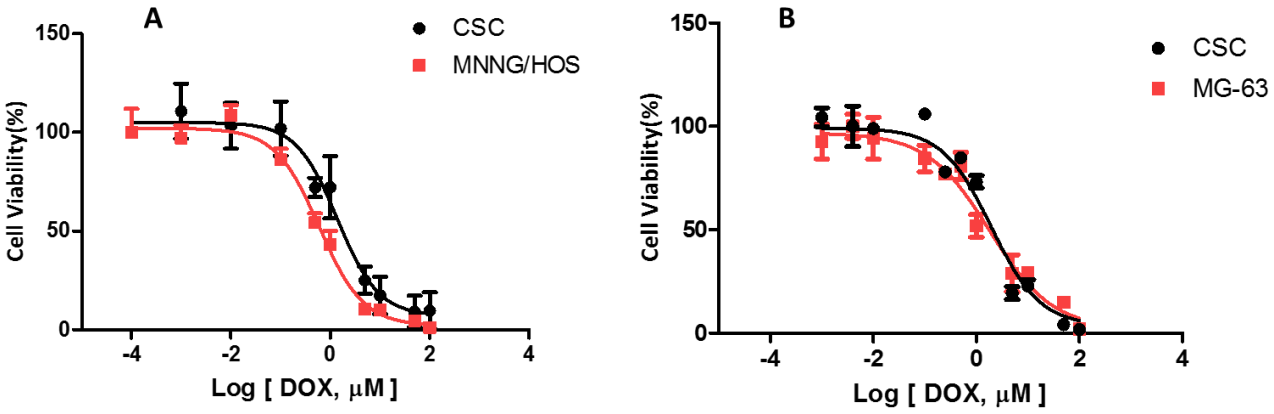

Figure 3.5. Representative dose-response curves for DOX in MNNG/HOS/CSCs (A) and MG-63/CSCs (B) fitted to a sigmoidal function.

The mean IC_{50} value for CSCs isolated from the MNNG/HOS cell lines was 1.96 ± 1.00 µM, significantly higher ($p<0.05$) than that estimated for parental cells (0.64 ± 0.19 µM) (Table 3.3). Regarding the MG-63 cell line, the IC_{50} values obtained for CSCs (1.97 ± 0.11 µM) was higher although not statistically significant as compared with that in parental cells (1.39 ± 0.25 µM) (Table 3.3).

Table 3.3. IC_{50} values of DOX in parental cell lines, MNNG/HOS and MG-63, and in corresponding CSCs.

	IC_{50} (μM)			
	MNNG/HOS	**CSCs**	**MG-63**	**CSCs**
DOX	0.64 ± 0.19 (n=6)	1.96 ± 1.00* (n=6)	1.39 ± 0.25 (n=3)	1.97 ± 0.11 (n=3)

Abbreviations: IC_{50}, half maximal inhibitory concentration; DOX, doxorubicin. Cells were incubated with increasing concentrations of DOX (0-100μM) during 48 hours. Cytotoxic effect was evaluated using the MTT colorimetric assay. The IC_{50} values were obtained from a sigmoidal fitting of the dose-response curves. Results are expressed as mean ± standard deviation (SD) of at least three independent assays performed in triplicate.
*$p < 0.05$ when compared with MNNG/HOS cells.

3.4. Effect of METF on DOX-induced cytotoxicity in parental cells and CSCs

Based on our previous observations that CSCs are more susceptible to METF than their differentiated counterparts, as indicated by the MTT and BrdU assays, we attempt to analyze the chemosensitizer effects of METF when administered in combination with DOX (a standard chemotherapeutic drug for OS) in what concerns cell viability. To further identify any potential synergy or additivity between DOX and METF we used different drug combinations. DOX was tested at three different concentrations equal, below and above the IC_{50} of parental cells (0.25 μM; 0.5 μM and 1 μM). Each of these DOX concentrations was combined with 0.05 mM, 0.1 mM, 1 mM, 2 mM and 5 mM of METF.

The effects of METF in combination with DOX on cell viability of MNNG/HOS and derived CSCs are presented in Figure 3.6 and Table 3.4. A chemosensitizing effect of METF was mainly observed when co-administered with the lowest tested concentration of DOX (0.25 μM), which by itself induced a slight decrease in cell viability to 78.41 ± 5.92 % in MNNG/HOS cells and of 92.42 ± 10.35 % in CSCs. The combination with METF increased the susceptibility of both parental MNNG/HOS and CSCs to DOX, as evidenced by the lower percentage of viable cells that decreased significantly in relation to the control (treated cells with 0.25 μM). This effect, in parental MNNG/HOS cells, was not very pronounced (although significant) and was maintained almost constant within the range of METF concentrations between 0.05 mM and 2 mM. For 5 mM of METF cell viability decreased to 34.82 ± 4.71 % which correspond to

relative percentage variation of 55.6 %. For concentrations of DOX of 0.5 µM or 1 µM, the chemosensitizing effects of METF were not significant except when used at 5 mM.

In CSCs, the chemosensitizing effect was also more evident when combined with 0.25 µM DOX. The decrease on cell viability was more pronounced and occurred in a dose-dependent manner (Figure 3.6 and Table 3.4). A dose of 2 mM or 5 mM of METF combined with 0.25 µM DOX decrease the percentage of viable CSCs to 63.07 ± 12.69 % and 9.38 ± 6.35 %, respectively, which corresponds to a relative percentage variation with respect to treated cells with 0.25 µM DOX of 31.7 % and 89.9 %, respectively. The same combination of drugs in MNNG/HOS cells resulted in a smaller relative percentage variation of 12.5 % and of 55.6 % (Table 3.4). When combined with higher concentrations of DOX, the chemosensitizing effect of METF was significant when used at the highest concentrations (2 mM and 5 mM).

The combination index (CI) obtained by using dose-response curves for each drug alone or in combination varied between 0.49 and 0.60 for METF concentrations inferior to 1 mM, indicating a strong to moderate synergistic effect. For METF concentrations equal or above 1 mM the CI emerge in the range of 0.85 and 0.95 indicating an addictive effect.

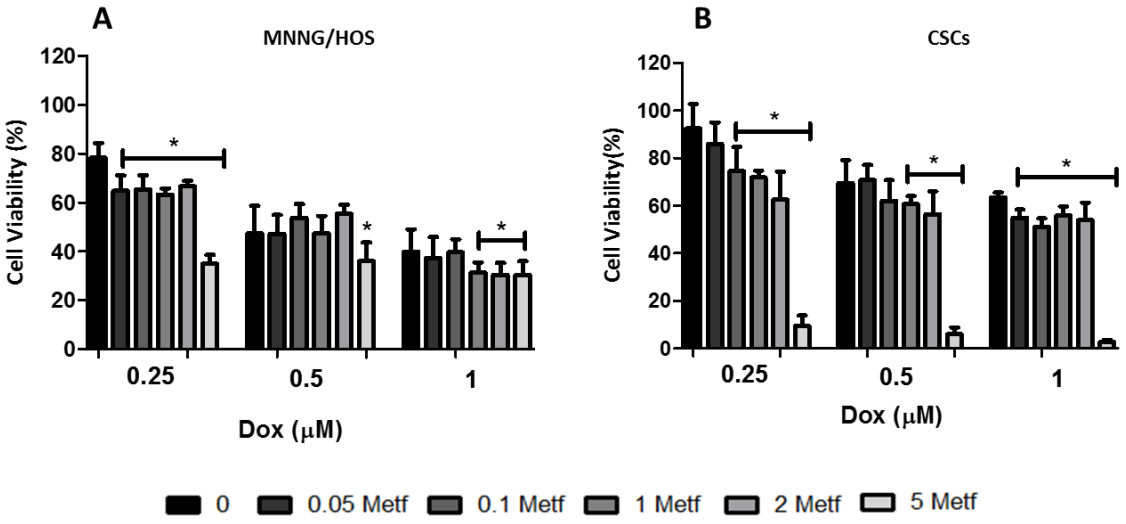

Figure 3.6. Percentage of viable cells after 48h of treatment with DOX (0.25µM, 0.5µM and 1 µM) in combination with different concentrations of METF (0.05mM-5mM) as assessed by the MTT assay in MNNG/HOS (A) and CSCs (B). The results were presented as mean ± standard deviation (SD) from three independent assays (n=3) performed in triplicate.
*p<0.05 when compared with control (treatment of DOX alone)

Table 3.4. Effects of METF on cytotoxicity of DOX in MNNG/HOS and CSCs.

Cell Viability (%) – MNNG/HOS											
Metf (mM)											
	0	*0.05*		*0.1*		*1*		*2*		*5*	
Dox (µM)			RPV		RPV		RPV		RPV		RPV
0.25	*78.41 ± 5.92*	65.81 ± 6.78 *	16.1%	66.14 ± 6.64 *	15.6%	64.81 ± 2.68 *	17.3%	68.60 ± 1.82 *	12.5%	34.82 ± 4.71 *	55.6%
0.50	*47.49 ± 11.25*	47.17 ± 7.82	0.67%	53.73 ± 5.72	-13.1%	47.47 ± 7.09	0.04%	56.63 ± 5.23	-19.2%	37.97 ± 9.50 *	20.0%
1.00	*39.90 ± 9.13*	36.56 ± 8.83	8.37%	38.45 ± 6.01	3.63%	31.23 ± 5.07 *	21.7%	32.42 ± 7.12 *	18.7%	30.12 ± 7.22 *	24.5%
Cell Viability (%) – CSCs											
Metf (mM)											
	0	*0.05*		*0.1*		*1*		*2*		*5*	
Dox (µM)			RPV		RPV		RPV		RPV		RPV
0.25	*92.42 ± 10.35*	85.35 ± 9.71	7.65%	74.56 ± 10.21*	19.3%	73.20 ± 2.70*	20.8%	63.07 ± 12.69 *	31.7%	9.38 ± 6.35*	89.9%
0.50	*68.89 ± 9.99*	70.07 ± 7.44	-1.71%	61.96 ± 9.99	10.1%	60.54 ± 4.34 *	12.1%	56.41 ± 9.64 *	18.1%	5.87 ± 3.49*	91.5%
1.00	*63.45 ± 3.24*	54.37 ± 4.10*	14.3%	53.13 ± 5.64 *	16.3%	55.79 ± 5.09 *	12.1%	54.12 ± 7.80 *	14.7%	2.48 ± 1.01*	96.1%

Abbreviations: METF, metformin; CSCs, Cancer Stem Cells; RPV, Relative Percentage Variation. Cells were incubated with DOX (0.25-1.0µM) in combination with increasing concentrations of METF (0-5mM) for 48 hours. Cytotoxicity was evaluated using the MTT colorimetric assay. Results are expressed as mean ± standard deviation (SD) of four (n=4; 0.05 and 0.1mM of METF in MNNG/HOS) and three (n=3) independent assays performed in triplicate.
*p<0.05 when compared with parental cell line (treatment of DOX alone)
The relative percentage variation (RPV) was calculated by dividing the difference on cell viability between DOX and DOX-METF treated cells by the viability of DOX treated cells.

The results obtained with the MG-63 cell line were similar to those observed with the MNNG/HOS cells. METF exerted a small chemosensitizing effect in cells treated with 0.25 µM DOX. The cytotoxic response of MG-63 cells to 0.5 µM or 1 µM of DOX was not significantly altered when administered in combination with METF, (except when administered at 5 mM) as indicated in Figure 3.7A and Table 3.5.

As shown in Figure 3.7B, a dose-dependent effect was observed in the viability of CSCs treated with DOX in combination with increasing concentrations of METF. This effect was abrupt and significant for a METF concentration equal or above 1 mM and was observed for all DOX concentrations tested, being the strongest effects achieved with 5 mM of METF (Figure 3.7B, Table 3.).

The CI values obtained from the Compusyn software identify a synergism between DOX and METF at concentrations between 0.05 and 1mM, with CI values between 0.62 and 0.85. For METF concentrations above 1 mM the CI values emerge in a range of 0.9 to 0.95 identifying an additive effect.

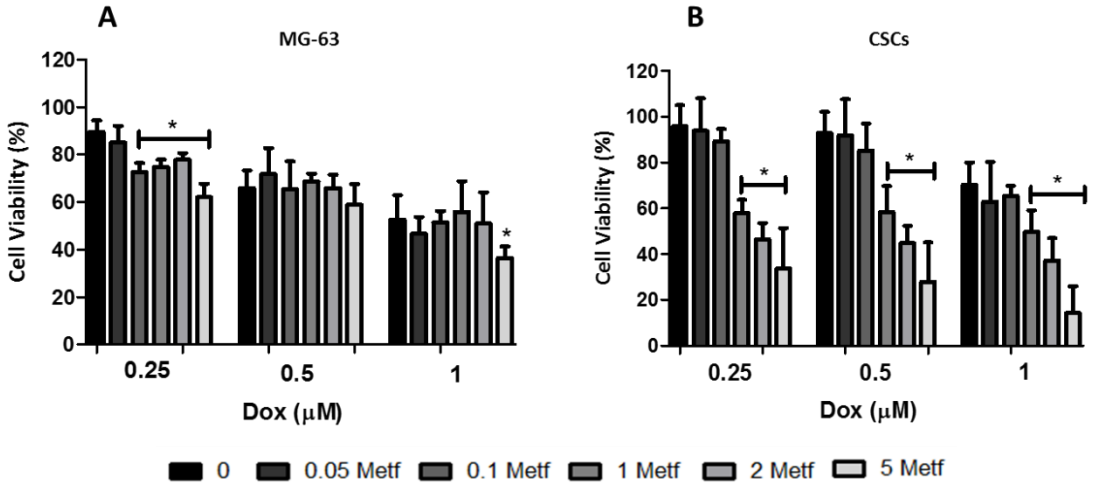

Figure 3.7. Percentage of viable cells after 48h of treatment with DOX (0.25μM, 0.5μM and 1 μM) in combination with different concentrations of METF (0.05mM-5mM) assessed by the MTT colorimetric assay in MG-63 (A) and CSCs (B). These results were presented as mean ± standard deviation (SD) from three independent assays (n=3) performed in triplicate.
*p<0.05 when compared with control (treatment of DOX alone)

Table 3.5. Effects of METF on cytotoxicity of DOX in MG-63 and CSCs.

Cell Viability (%) – MG-63											
Metf (mM)											
	0	***0.05***		***0.1***		***1***		***2***		***5***	
Dox (μM)			RPV		RPV		RPV		RPV		RPV
0.25	***89.10 ± 5.08***	84.95 ± 7.41	4.66%	73.62 ± 5.56 *	17.4%	74.36 ± 3.89 *	16.5%	79.24 ± 3.06 *	11.1%	62.03 ± 5.69 *	30.4%
0.50	***65.19 ± 8.11***	72.43 ± 16.25	- 11.1%	68.68 ± 14.64	- 5.35%	70.00 ± 4.01	- 7.38%	65.91 ± 6.05	- 1.10%	58.95 ± 8.66	9.57%
1.00	***52.68 ± 10.25***	46.29 ± 7.74	12.1%	51.49 ± 5.09	2.26%	55.89 ± 13.00	- 6.09%	51.09 ± 13.06	3.02%	36.16 ± 5.19 *	31.4%
Cell Viability (%) – CSCs											
Metf (mM)											
	0	***0.05***		***0.1***		***1***		***2***		***5***	
Dox (μM)			RPV		RPV		RPV		RPV		RPV
0.25	***95.39 ± 9.59***	93.68 ± 15.29	1.79%	89.79 ± 5.50	5.87%	58.36 ± 6.03*	38.8%	46.48 ± 7.11 *	51.3%	35.51 ± 17.96*	62.8%
0.50	***93.33 ± 9.78***	91.73 ± 16.84	1.71%	85.30 ± 12.64	8.60%	58.42 ± 11.29*	37.4%	44.82 ± 7.51 *	52%	27.91 ± 17.19*	70.1%
1.00	***70.24 ± 9.83***	63.59 ± 19.19	9.47%	65.95 ± 5.65	6.11%	49.71 ± 9.41*	29.2%	37.22 ± 9.71 *	47.0%	14.31 ± 11.60*	79.6%

Abbreviation: METF, metformin; CSCs, Cancer Stem Cells; RPV, Relative Percentage Variation. Cells were incubated with DOX (0.25-1.0μM) in combination with increasing concentrations of METF (0.05-5mM) for 48 hours. Cytotoxicity was evaluated using the MTT colorimetric assay. These results were presented as mean ± standard deviation (SD) from three independent assays (n=3) performed in triplicate.
*p<0.05 when compared with parental cell line (treatment with DOX alone).
The relative percentage variation (RPV) was calculated by dividing the difference on cell viability between DOX and DOX-METF treated cells by the viability of DOX treated cells.

3.5. Effect of METF on sphere-formation and self-renewal of CSCs

After verifying that CSCs are more susceptible to METF than parental cells, next we evaluated the effect of different concentrations of METF on sphere formation and self-renewal ability of CSCs, by conducting a sphere forming assay, using monolayer parental cells and dissociated cells from first generation spheres, respectively. We found that METF within the range of concentrations tested did not induce significant alterations on the sphere forming efficiency of MNNG/HOS cells as represented in the graph of Figure 3.8 A. However, as shown in the images of Figure 3.8 A, the size of the spheres formed at higher concentrations of METF (2mM and 5mM) were smaller and less compact compared with untreated cells. Regarding self-renewal ability, we observed that METF at 2 mM and 5 mM decreased significantly the number of secondary sarcospheres compared with untreated cells, as depicted in Figure 3.8 B. For 1 mM of METF the formed spheres are smaller and for 2 mM and 5 mM, revealed morphology more likely to be cellular aggregates with irregular contours and not real spheres as observed in controls or cells treated with low concentrations of METF, as shown in Figure 3.8 B.

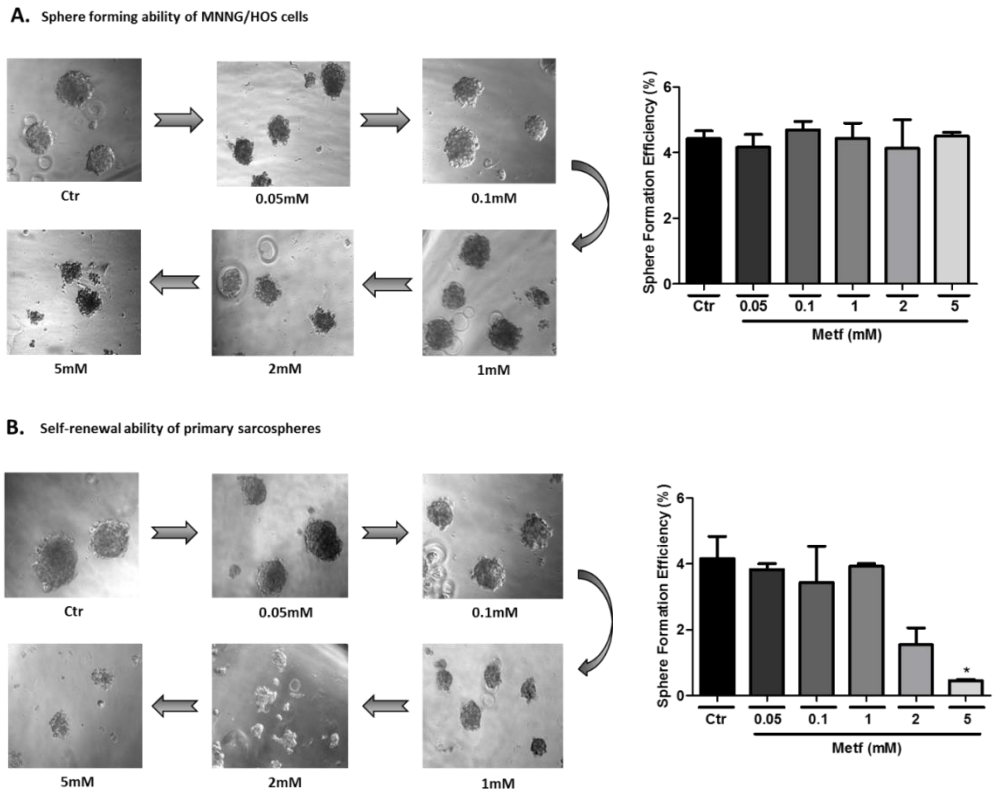

Figure 3.8. Effects of METF on sphere formation and self-renewal ability of MNNG/HOS cells. (A) Morphological appearance and sphere-forming efficiency of MNNG/HOS cells treated with METF at indicated concentrations. (B) Self-renewal ability of primary generation sarcospheres in the presence of METF. These results were presented as mean ± standard error of the mean (SEM) from three independent assays (n=3).
*p<0.05 when compared with parental cells (untreated)

The results obtained with the MG-63 cells were similar to those obtained with the MNNG/HOS cell line. METF decreased the sphere-forming efficiency in both primary and secondary sarcospheres for concentrations of 2mM or 5mM of METF. Likewise, the size of spheres was smaller than those formed in medium without METF. With the increasing concentrations of METF, the sizes of the spheres decreased and start losing the appearance of round colonies acquiring a morphology of cellular aggregates mainly for the highest concentrations as shown in the Figure 3.9 A and B.

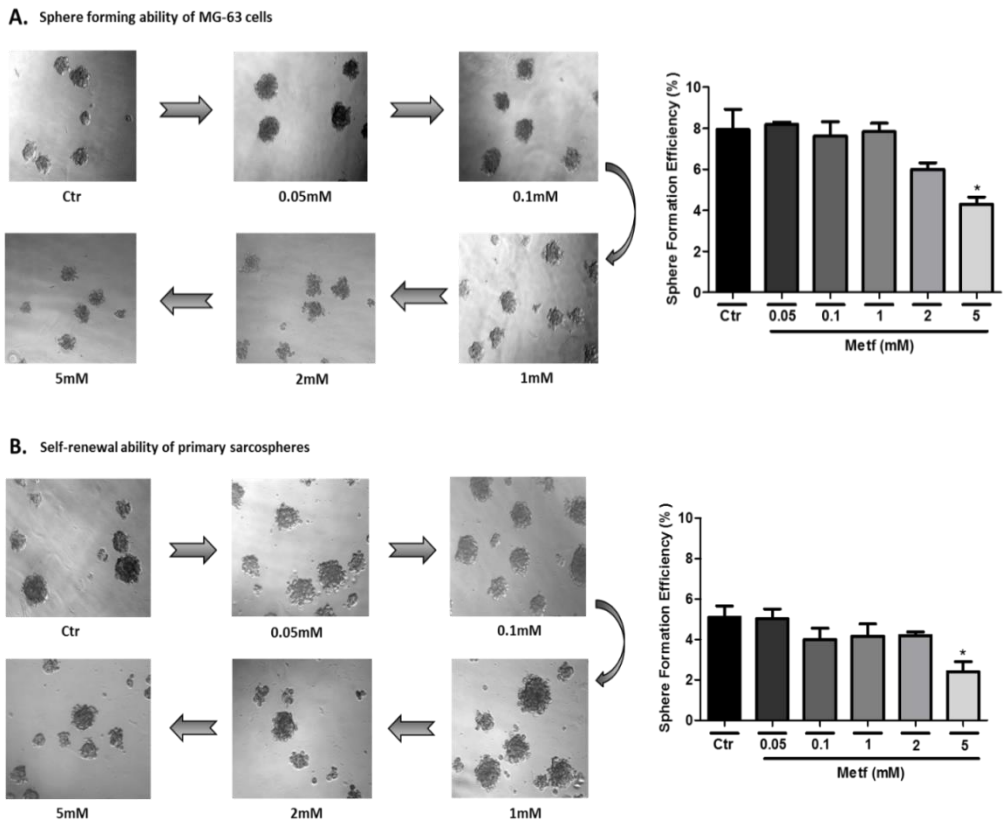

Figure 3.9. Effects of METF on sphere formation and self-renewal ability of MG-63 cells. (A) Morphological appearance and sphere-forming efficiency of MG-63 cells treated with METF at indicated concentrations. (B) Self-renewal ability of primary generation sarcospheres in the presence of METF. These results were presented as mean ± standard error of the mean (SEM) from three independent assays (n=3).
*p<0.05 when compared with parental cells (untreated)

3.6. Activation of sensors of energetic status of the cell by METF in parental cells and corresponding CSCs

3.6.1. Expression of activated AMPK in parental cells and corresponding CSCs

The main mechanism of anti-neoplastic action by METF has been attributed to the activation of AMPK, which is a cellular energy sensor involved in regulating cellular metabolism and proliferation. Once activated, METF downregulates energy consuming processes (e.g. protein synthesis and proliferation) and upregulates processes that lead to ATP synthesis (e.g. glucose uptake). Based on this assumption we evaluated the expression levels of the activated form of AMPK in both parental cells and corresponding derived CSCs after 48h cells exposure to METF over a range of concentrations between 0.05 mM to 2 mM.

It was not possible to test the effects of 5mM METF because of the very small amount of protein obtained.

Western blot analysis showed a progressive increase in *AMPK*-α *phosphorylation* levels (pAMPK) with increasing concentrations of METF, in both parental MNNG/HOS and MG-63 cells and corresponding CSCs, becoming significant for 2 mM, whereas the total AMPK remained almost unchanged as indicated in Figures 3.10 and 3.11. Nevertheless, METF-induced AMPK activation appeared most pronounced in both CSCs populations as compared to respective parental cells (Figures 3.10B and 3.11B), further suggesting that CSCs are more sensitive than parental cells to METF-induced AMPK activation.

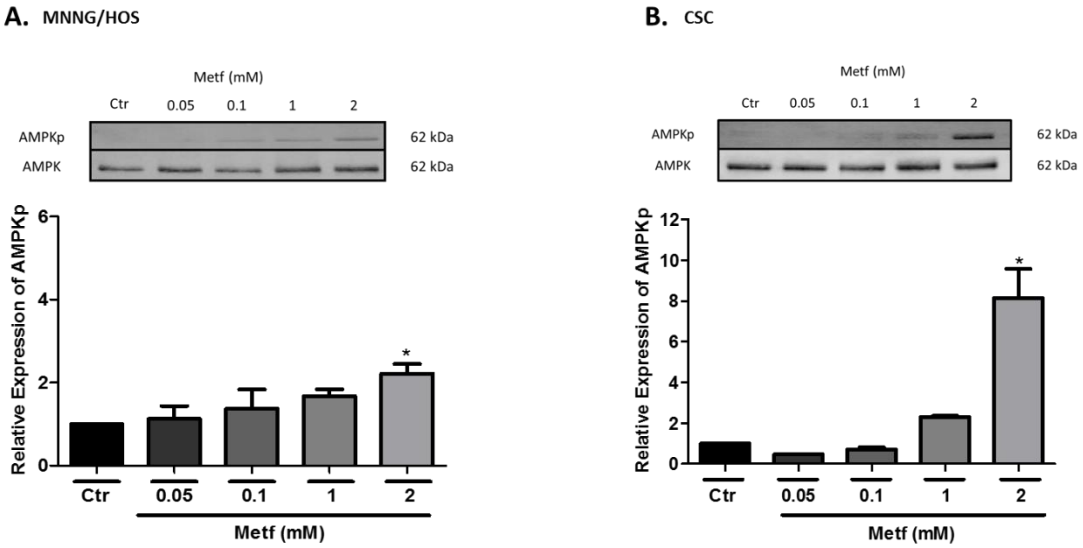

Figure 3.10. Representative Western Blot analysis of pAMPK expression levels in MNNG/HOS (**A**) and corresponding CSCs (**B**) after incubation with increasing concentrations of METF during 48 hours. The graphs below show the quantitative analysis of pAMPK levels normalized to the total AMPK and expressed as a ratio of the levels found in untreated cells (control). These results were presented as mean ± standard error of the mean (SEM) from four independent assays (n=4).
*p<0.05 when compared with control (untreated)

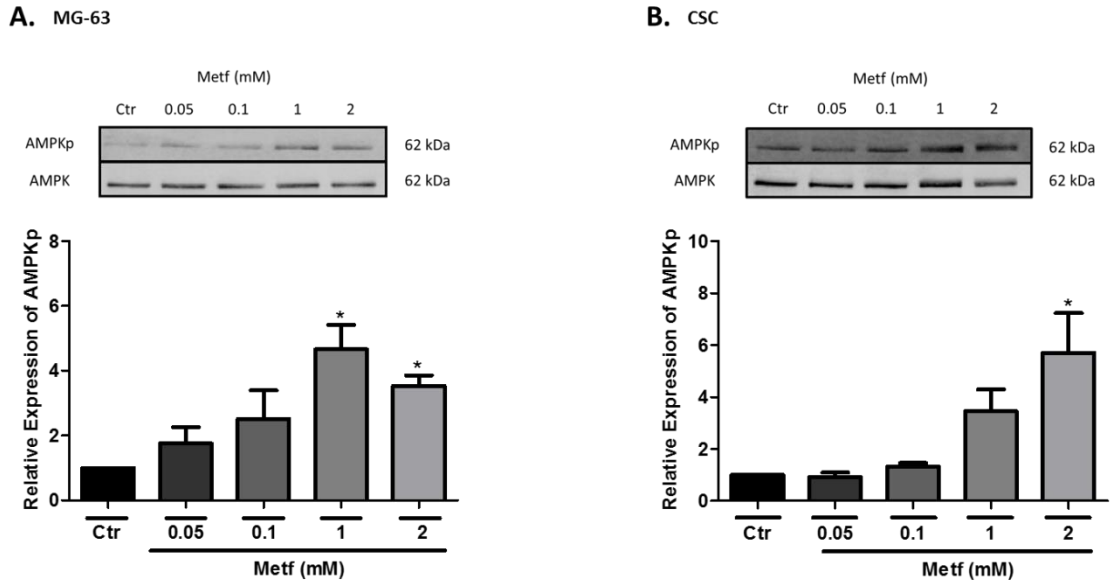

Figure 3.11. Representative Western Blot analysis of pAMPK expression levels in MG-63 (**A**) and corresponding CSCs (**B**) after incubation with increasing concentrations of METF during 48 hours. The graphs below show the quantitative analysis of pAMPK levels normalized to the total AMPK and expressed as a ratio of the levels found in untreated cells (control). These results were presented as mean ± standard error of the mean (SEM) from five and four independent assays, respectively (n=5 for MG-63 and n=4 for CSCs). *p<0.05 when compared with control (untreated)

3.6.2. Expression of the downstream target (mTOR) of activated AMPK in parental cells and corresponding CSCs

The suppression of mTOR activity through AMPK activation is believed to constitute the major mechanism underlying the anti-cancer activities of METF. Therefore we evaluated the expression levels of mTOR following exposure to METF verify whether AMPK activation induce a concomitant mTOR inhibition. This analysis was performed by Western blot only once and the results are presented in Figure 3.12 and 3.13.

The expression levels of mTOR in parental MNNG/HOS treated with 0.1mM or 1mM of METF increased 2-3 fold, in relation to untreated cells, but remained almost constant for the other METF tested concentrations (Figure 3.12 A). In corresponding CSCs, the mTOR expression levels decreased to less than half in relation to the control and remained almost constant irrespective of the METF concentrations as depicted in Figure 3.12 B.

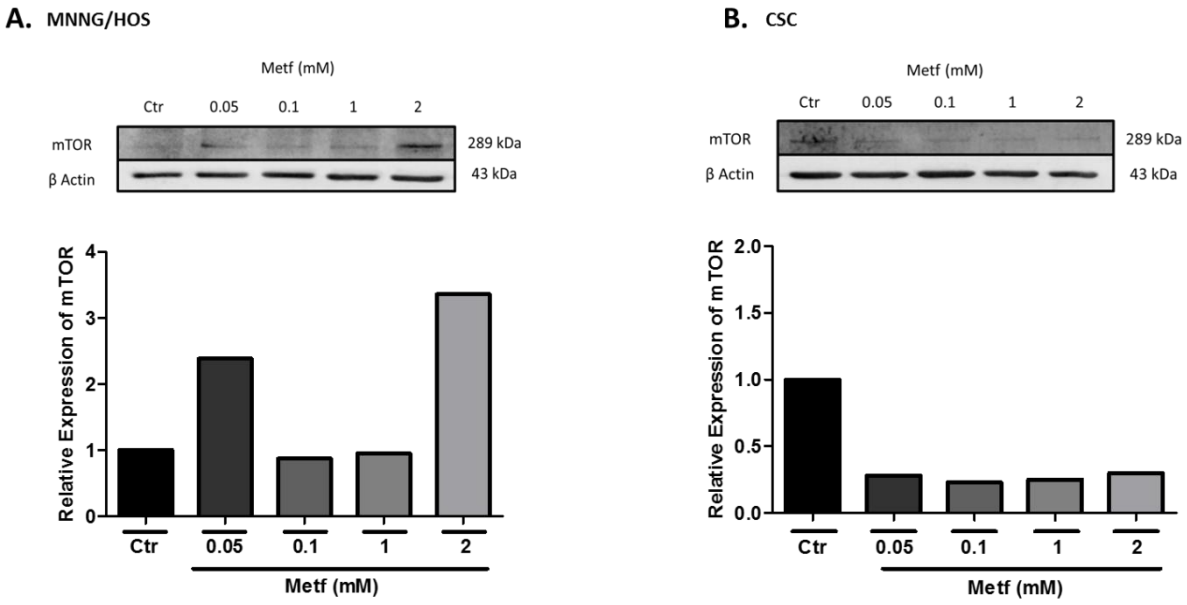

Figure 3.12. Representative Western Blot analysis of mTOR expression levels in MNNG/HOS (**A**) and corresponding CSCs (**B**) after incubation with increasing concentrations of METF during 48 hours. The graphs show the quantitative analysis of mTOR levels normalized to β Actin and expressed as a ratio of the levels found in untreated cells (control) (n=1).

The expression levels of mTOR in parental cell line MG-63 decreased slightly for treatments with 0.05 mM or 0.1 mM of METF and increased at concentrations of 1 mM or 2 mM as demonstrated in Figure 3.13 A. In the case of MG-63-derived CSCs there were no significant changes in the expression levels of mTOR expression, with the treatment of METF, suggesting they are more resilient to the effect of METF in the reduction of mTOR levels, compared with MNNG/HOS-derived CSCs.

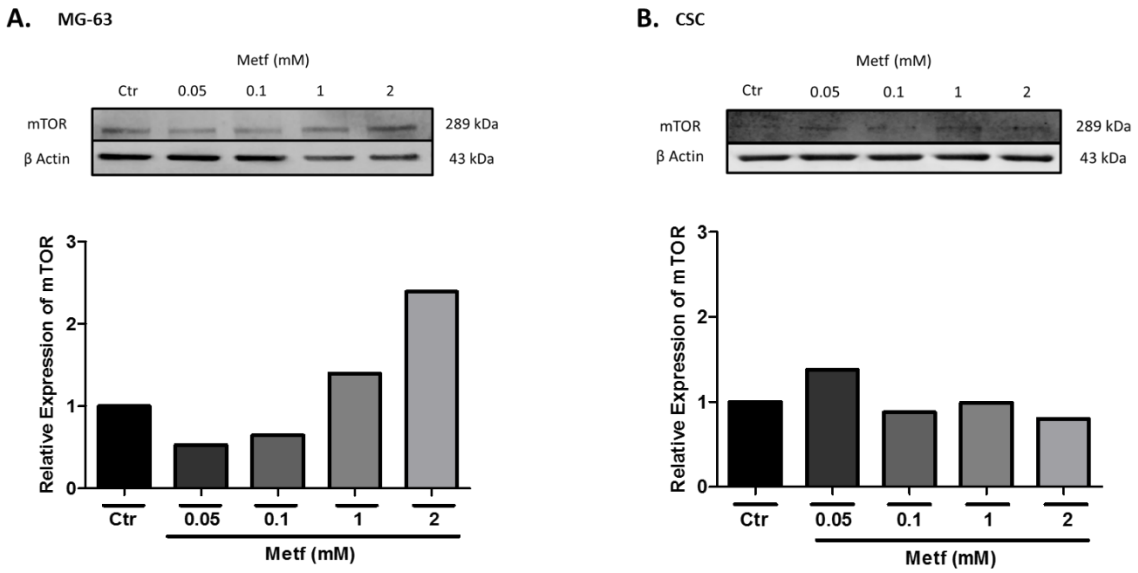

Figure 3.13. Representative Western Blot analysis of mTOR expression levels in MG-63 (**A**) and corresponding CSCs (**B**) after incubation with increasing concentrations of METF during 48 hours. The graphs below show the quantitative analysis of mTOR levels normalized to β Actin and expressed as a ratio of the levels found in untreated cells (control) (n=1).

3.7. Effects of METF on metabolic activity of parental cells and CSCs

One of the effects of METF is to upregulate processes that lead to ATP synthesis including glucose uptake, secondary to activation of AMPK. Therefore we measure the cellular uptake of [^{18}F]FDG, a glucose analogue radiotracer in both parental and CSCs after treatment with various concentrations of METF at a maximum of 2 mM. Is was not possible to test the effects of 5mM of METF because of the few number of adherent surviving cells which hindered the execution of the assay.

A progressive and dose-dependent increase in [^{18}F]FDG uptake was observed in both parental MNNG/HOS and MG-63 cells, although the effects are more pronounced in MNNG/HOS cells as depicted in Figure 3.14 and Table 3.6.

In MNNG/HOS cells the cellular uptake of [^{18}F]FDG increased 8-fold and 20-fold when treated with 1mM or 2 mM of METF, respectively in relation to untreated cells, whereas in MG-63 cells the increase was of 1.6 and 2.4-fold under the same conditions. These differences on metabolic response to METF between MNNG/HOS and MG-63 cells, can be related with other mechanisms regulating [^{18}F]FDG uptake.

As shown in Figure 3.14, METF had no noticeable effects on the metabolic activity of CSCs, since no significant changes were observed in [^{18}F]FDG uptake following treatment with METF, suggesting that METF may not overtake the quiescent status of CSCs and consequent lower energy requirements.

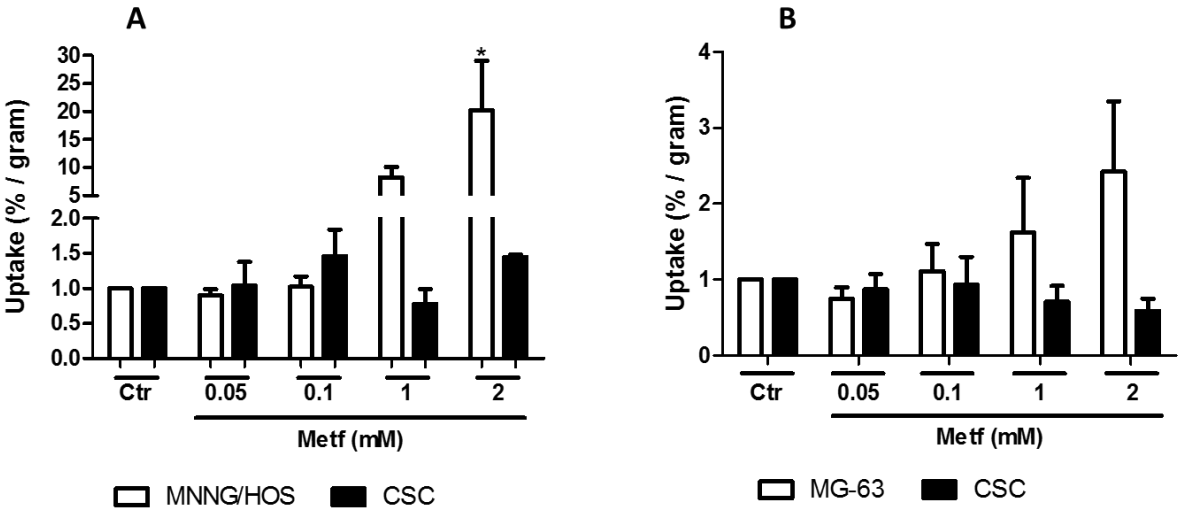

Figure 3.14. Uptake of [^{18}F]FDG after treatment with different concentrations of METF (0.05-2mM), for MNNG/HOS cell line and corresponding CSCs (A) and in MG-63 cell line and corresponding CSCs (B). These results were presented as mean ± standard error of the mean (SEM) from three independent assays (n=3) performed in triplicate for both parental cell lines and corresponding CSCs.
*p<0.05 when compared with control (untreated)

Table 3.6. [^{18}F]FDG Uptake after treatment with different concentrations of METF in both parental cell lines (MNNG/HOS and MG-63) and corresponding CSCs.

	Uptake FDG (% / gram)			
METF (mM)	**MNNG/HOS**	**CSC**	**MG-63**	**CSC**
0	1.00 ± 0.00	1.00 ± 0.00	1.00 ± 0.00	1.00 ± 0.00
0.05	0.90 ± 0.09	1.04 ± 0.34	0.75 ± 0.15	0.87 ± 0.20
0.1	1.02 ± 0.15	1.46 ± 0.38	1.11 ± 0.36	0.93 ± 0.37
1	8.25 ± 1.88	0.78 ± 0.21	1.62 ± 0.72	0.71 ± 0.21
2	20.26 ± 8.83 *	1.45 ± 0.03	2.42 ± 0.93	0.59 ± 0.16

Abbreviation: METF, metformin; CSCs, Cancer Stem Cells. Cells were incubated with increasing concentrations of METF (0-2mM) for 48 hours. Data are displayed relative to respective controls (untreated cells). These results were presented as mean ± standard error of the mean (SEM) from three independent assays (n=3).
*p<0.05 when compared with control (untreated)

CHAPTER 4

DISCUSSION

In this study we purpose to evaluate the potential role of METF as co-adjuvant when used in combination with DOX in the treatment of OS targeting CSCs that are believed to play a critical role in drug resistance and tumor progression.

METF is a widely used and well tolerated drug prescribed to treat patients with type II diabetes. This drug has recently received particular attention for its potential anti-cancer properties due to anti-proliferative effects on tumor cells and anti-tumor growth effects in mouse xenografts suggesting the possibility of its use as an anticancer agent in non-diabetic contexts [84]. We attempt to evaluate the cytotoxicity of METF towards drug-resistant CSCs existing in OS, in combination with DOX, which is the main chemotherapeutic agent used in the treatment of OS.

Previous studies performed in our group have demonstrated the presence of a subpopulation of cells exhibiting stem-like properties in a human OS cell line (MNNHG/HOS) that were relatively resistant to chemotherapeutic drugs (including DOX) and radiotherapy as compared to their differentiated counterparts [19]. In this study we have identified a stem-like cell population in another human OS cell line (MG-63), using the same functional approach based on the sphere-forming assay, which is a recognized and currently used method for identifying CSCs in solid tumors [36]. Under serum-starvation and anchorage-independent conditions only cells with stem-like properties can survive forming suspended spherical colonies while more differentiated cells are unable to survive in these stressful conditions being eliminated. We observed that MG-63 cells likewise MNNG/HOS formed spherical colonies for at least four generations under these stressful culture conditions which is indicative of their self-renewal ability, a hallmark of CSCs. Furthermore, when transferred into adherent flasks with serum containing standard growth medium, CSCs expanded in monolayer and generated progeny with the same morphological phenotype of the parental cell line, demonstrate their differentiation ability, another CSCs property.

To further confirm the stem-like nature of the isolated CSCs, we analysed the expression of Oct4 and Nanog, two core regulatory transcription factors required for maintaining pluripotency and self-renewal of embryonic stem cells (ESCs). The immunofluorescence staining showed that both Oct4 and Nanog are expressed in CSCs derived from the MNNG/HOS and MG-63 cells, and are localized in both the nuclei and the cytoplasm of cells while no immunoexpression were found in parental cells. The localization of transcription factors in the cytoplasm suggests that they might display other function in CSCs distinct of self-renewal regulation. Recent data demonstrated that ESCs-associated proteins are highly

expressed in different tumors and contribute to tumor aggressiveness and poor outcome, by promoting tumor cell growth, anti-apoptosis and invasiveness, which are the typical characteristics associated to CSCs [103], however their exact role are not fully understood. In previous work the protein expression levels of Oct4 and Nanog were found highly elevated in MNNG/HOS-derived CSCs compared with parental cells as determined by Western blot [19]. Other authors in independent studies demonstrated the expression of these markers in cancer stem-like cells isolated from bone and soft-tissue sarcomas confirming the higher expression of Oct4 and Nanog in sarcospheres than adherent cells [14, 36]. Levings and collaborators (2009) through *in vivo* transplantation demonstrated that a small number of cells expressing Oct4 could amplify and increase the expression or activation of Oct4 representing a >100-fold enrichment of tumorigenic capacity in OS, which represents other function of Oct4 than regulatory of pluripotency. This marker was found to be only active in TICs and not in the normal MSCs or in the more differentiated osteoblast cell line [105].

The dose-response studies to DOX confirmed the high resistance profile of the CSCs populations to this drug, as indicated by the IC_{50} values taken from the dose-survival curves obtained after 48h incubation with DOX (Figure 3.5 and Table 3.3).

Regarding CSCs derived from the MNNG/HOS cell line, the IC_{50} (IC_{50} = 1.96 ± 1.00 μM) was 3-fold higher than that observed for parental MNNG/HOS cells (IC_{50} = 0.64 ± 0.19 μM). Relatively to the MG-63 cell line, the IC_{50} was 1.4-fold higher in CSCs (IC_{50}= 1.97 ± 0.11 μM) than in parental cells (IC_{50} = 1.39 ± 0.25 μM). One mechanism that has been proposed to explain the chemoresistance of CSCs is the activity of ABC transporters that mediate drug efflux, preventing the cellular accumulation of chemotherapeutic agents. DOX is a transport substrate of Pgp and BCRP, two transmembrane efflux transporters that have been found to be overexpressed in CSCs of several malignancies, namely breast, hepatocellular, gastrointestinal and thyroid cancers [62]. These proteins behave as drug efflux pumps preventing the intracellular accumulation of DOX at toxic levels and confer a multidrug resistance phenotype and are associated with drug resistance, tumor recurrence and poor outcome in OS patients [106, 107]. Previous studies conducted in our lab demonstrated high expression levels of Pgp and BCRP in CSCs derived from the MNNG/HOS cell line, which might explain the higher resistance of such CSCs to DOX [19]. Additionally, verapamil (VER) co-administration, a non-specific inhibitor of ABC transporters, sensitized CSCs to DOX and had no significant effects on parental cells further suggesting that both transporters are functionally active and contribute to DOX resistance of CSCs. Furthermore, studies conducted

in our laboratory showed that the increased resistance of MNNG/HOS-derived CSCs to DOX-inducing apoptosis was related with the disruption of intrinsic or mitochondrial apoptotic pathway demonstrated by an upregulation of anti-apoptotic proteins and a downregulation of pro-apoptotic proteins in these cells [82].

Before examining the anticancer properties of METF together with DOX, we first analysed the effects of METF by itself on cell viability and proliferation using the MTT and BrdU incorporation assays, respectively, in a concentration ranging between 0.05 mM and 5 mM. Most of the studies found in the literature use much higher concentrations of METF (typically between 5mM and 30 mM) than the recommended doses for clinical use (30-50 nM), since in most cases little or no effects on cell proliferation are observed at these low concentrations. Our results showed that METF induced a decrease in cell viability and proliferation in both parental cells and corresponding CSCs populations, for concentrations equal or above 1mM. For lower METF concentrations within the range of clinically therapeutic doses, the effects were not significant. However in both cell lines (MNNG/HOS or MG-63), the effects of METF either on viability or proliferation were more pronounced in the CSCs populations. These results are in accordance with those reported in studies performed in thyroid and pancreatic CSCs. In these studies it was observed a decrease in cell proliferation follow METF treatment [88, 94]. Another study performed in breast CSCs show that METF was preferentially cytotoxic to CSCs relatively to non-CSCs, however the mechanism underlying this effect is not well understood yet [108].

The potential benefits of METF as an anticancer agent are believed to be mediated by the activation of AMPK which plays a major role in the regulation of energetic metabolism and proliferation in tumor cells. This drug activates the AMPK pathway because of the inhibition of mitochondrial complex I. This alteration in mitochondria activity causes an alteration in AMP/ATP ratio that results in AMPK activation, which in turn suppresses the activity of mTOR, a signaling pathway clinically relevant to cancer that plays a central role in regulating cell growth by controlling mRNA translation and ribosome biogenesis. The activated form of AMPK inhibits the mTOR activity via phosphorylation and stabilization of the tumor suppressor TSC2 a subunit of the TSC2/TSC1 complex that negatively regulates mTOR signaling or through direct phosphorylation of co-signaling molecules that bind to mTOR and inhibit its action [85].

We examined the expression levels of phosphorylated AMPK to further verify if the activation of AMPK is responsible for the effects of METF observed in OS cells, and in fact we observed an increase in AMPK phosphorylation in both parental MNNG/HOS and MG-63 cell lines as well as in the corresponding subpopulations of CSCs in a dose-dependent manner. However the AMPK activation appears to be more pronounced in CSCs than in their counterparts suggesting that CSCs are more sensitive to METF-induced AMPK activation. Contrary to what is described in the literature we did not observe a significant concomitant decrease in mTOR expression in any of the cell lines tested, further suggesting that METF at the tested concentrations reduces cell proliferation through an independent mechanism of mTOR activity. However, the measurement of the expression levels of mTOR was only performed one time, and should be confirmed through repeated experiments.

The anticancer effects of METF has been evaluated in several types of cancer, namely endometrial, breast, pancreatic and lymphoma and it was shown to be related with AMPK activation and subsequent mTOR inhibition. In endometrial cell lines mTOR inhibition leads to suppression of proliferation through cell cycle arrest, whereas in breast cancer cell lines, the decrease in cell growth was due to the inhibition of mTOR and to a decrease in phosphorylation of its downstream targets with a reduction in translation initiation [87, 92].

We cannot exclude other effects of METF independent of AMPK activation can afford the results observed in our study. Sahra *et al.* (2008) show that METF exerts an antiproliferative effect in prostate cell lines trough cell cycle arrest in G_0/G_1 phase which is correlated with a decrease in the expression of cyclin D1, E_2F1 and phosphorylation of pRb. Furthermore, these effects were accompanied by a downregulation of the mTOR pathway but independently of AMPK activation, since the inhibition of AMPK did not prevent the G_0/G_1 cell cycle arrest induced by METF [89]. Moreover, studies performed by Memmott *et al.* (2010) in lung cancer support the hypothesis that METF decrease cancer cell proliferation by decreased phosphorylation of IGF-1R and decrease levels of circulating IGF-1 and insulin [95]. Furthermore, in thyroid cancer cells were shown that METF could inhibits insulin/IGF signaling apart from AMPK/mTOR pathway [94].

Cancer cells preferentially use glycolysis to generate energy, releasing lactate from the cell despite the abundance of oxygen, in a phenomenon referred to as “the Warburg effect” [111]. As already mentioned, the AMPK complex functions as a metabolic checkpoint which regulates the cellular response to energy availability. During periods of energetic stress, AMPK becomes activated in response to an increased AMP/ATP ratio and is responsible for

shifting cells towards a more oxidative metabolic phenotype [112]. The activation of AMPK downregulates many of the energy-consuming activities of cells, including protein synthesis and cellular proliferation; also up-regulates pathways for energy production, such as glycolysis and fatty acid oxidation, and induce externalization of glucose transporters.

To further evaluate if METF induces differential effects in metabolic status between parental and CSCs, we measure the cellular uptake of [^{18}F]FDG following exposure to METF. [^{18}F]FDG is a glucose analogue used in the clinical practice in PET imaging studies to detect malignant tumors [113]. This radiotracer accumulates preferentially in tumor cells due to their high metabolic activity and energy requirements and is considered a good indicator of the metabolic status of tumor cells. The increased accumulation of [^{18}F]FDG in tumor cells in relation to non-tumor cells is attributed to an increase in the activity of enzymes that regulates glucose metabolism, such as hexokinase, and also due to the overexpression of glucose transporter proteins, such as GLUT-1 and GLUT-3 in tumor cells [97]. Our results showed that METF induced a progressive and dose-dependent increase in [^{18}F]FDG uptake in parental cells but not in CSCs that exhibited a constant [^{18}F]FDG uptake along the METF concentrations tested (Figure 3.14) .

We know from previous studies that CSCs are less glycolytic than differentiated OS cells, probably related with their quiescent status and consequent low energy requirements, which make them less susceptible to the effects of metabolic modulators METF in contrast with highly proliferative cells that rely more on glycolysis than on oxidative phosphorylation for glucose metabolism [19]. Würth *et al.* (2013) in a similar study performed in glioblastoma cells lines also observed significant differences in [^{18}F]FDG uptake between differentiated cells and CSCs in response to METF. CSCs have not responded to [^{18}F]FDG uptake comparing to their glioblastoma cancer cells which increase the [^{18}F]FDG uptake following METF treatment [115].

On the basis of our observations that METF exerted a more selective effect against CSCs, we evaluated the effect of METF in sphere forming and self-renewal abilities of both subpopulations of CSCs. We found that METF at higher concentrations (2 mM and 5 mM) impaired the sphere forming efficiency and reduced the sphere size of both primary and secondary sarcospheres, which reflects suppression of self-renewal and proliferation of CSCs. These results are in accordance with those reported by Bao *et al.* (2011) in CSCs isolated from pancreatic cancer cells. In addition to a decrease in proliferation of CSCs, they observed that METF decreased the sphere forming ability of CSCs by lowering the expression of CSCs marker

genes, such as CD44, EpCAM, Nanog and Oct4 [88]. A reduction in sphere formation and sphere size was equally observed in thyroid carcinoma CSCs at similar doses of METF [94]. Taken together these results suggest that METF modulates CSCs-specific genes linked with self-renewal capacity of cancer stem-like cells.

The Wnt/β-catenin is a developmental signaling pathway involved in the maintenance of the self-renewal capacity of stem/progenitor cells through the inhibition of terminal differentiation. This signaling pathway is deregulated in a variety of cancers and is considered an essential pathway in driving CSCs self-renewal and maintenance of their tumorigenic phenotype. Recent studies suggest that METF affects osteoblasts differentiation through modulation of the Wnt/β-catenin signaling pathway, by reducing the protein levels of β-catenin, which is the downstream effector of canonical Wnt signaling in osteoblast like-cells.

Takatani *et al.* (2011) showed that activation of AMPK by METF suppresses the transcriptional activity of the Wnt/β-catenin signaling pathway in an OS cell line by promoting the phosphorylation of β-catenin and its consequent degradation, further suggesting a cross-talk between AMPK and Wnt/β-catenin signaling [100].

Unpublished data obtained in our lab revealed a strong nuclear accumulation of β-catenin (the hallmark of active canonical Wnt signaling pathway) in CSCs-enriched cell populations isolated from the OS cell lines that we used in this study (MNNG/HOS and MG-63), while parental cells displayed only a membranous staining pattern, suggesting that Wnt/β-catenin signaling is required for the maintenance of CSCs. This information together with interplay between AMPK and the Wnt/β-catenin signaling pathway suggests that METF might impair the self-renewal capacity of CSCs through AMPK-mediated inhibition of the canonical Wnt signaling pathway.

Taking in consideration the previous observations that CSCs are more susceptible to METF but more resistant to DOX treatment, we attempted to analyse the chemosensitizer effect of METF when combined with DOX at cytostatic (below IC_{50}) and cytotoxic (above IC_{50}) concentrations. In fact, by the MTT assay we observed that METF potentiated the cytotoxic effects of DOX in both parental and CSCs populations, but with a more pronounced effect on CSCs. This chemosensitizing effect of METF was more effective when combined with a cytostatic concentration of DOX (below the IC_{50}), that *per se* exerted a low cytotoxicity against resistant CSCs, and was dose-dependent, being synergistic for relatively lower doses of METF (< 1mM) and additive for doses equal or above 1 mM. Moreover, the chemosensitizing effect of METF did not increased substantially when combined with higher concentrations of DOX,

suggesting that METF is effective in combination with reduced dosages of DOX and presumably other standard chemotherapeutic drugs.

METF has been shown to potentiate the cytotoxic action of some chemotherapeutic agents including DOX. Iliopoulos *et al.* (2011) and Hirsch *et al.* (2009) showed that administration of METF together with a reduced dosage of DOX is highly effective in blocking tumor growth and preventing relapse in a variety of cancer cell types. Furthermore, they observed that combination of METF with higher concentrations of DOX did not translate into an additional decrease in cell viability. Thus, METF appears to increase the effectiveness of standard chemotherapy and lowering the cytotoxic side-effects associated with chemotherapy in the clinical context [99,101].

Our results demonstrating a preferential cytotoxicity of METF against CSCs in OS, either alone or in combination with DOX are exciting and looks promising in the treatment of OS. However given the diversity of molecular targets and mechanisms of METF action, further studies are needed for a better understanding and elucidation of the molecular mechanisms underlying the preferential cytotoxicity of METF against CSCs in OS.

CHAPTER 5

CONCLUSION

In this study we purpose to explore the anticancer properties of METF as co-adjuvant of DOX in the treatment of OS targeting CSCs. Our results demonstrated that both OS cell lines contain a subpopulation of cells exhibiting stem-like features that can be isolated through the sphere formation assay.

The CSCs subpopulations are relatively more resistant to DOX than their differentiated adherent counterparts.

MEFT demonstrated a preferential cytotoxicity against CSCs relatively to corresponding parental cells through inhibition of cell viability and proliferation.

Treatment with METF resulted in activation of AMPK in both cell populations and interferes with glucose metabolism in proliferating parental cells, but not in CSCs.

METF potentiates the cytotoxic effects of low doses DOX (below the IC_{50}) preferentially in CSCs.

In conclusion, our results suggest that METF combined with DOX may be an effective treatment strategy for targeting CSCs in OS, however more studies are needed to clarify the mechanisms underlying the chemosensitizing effects of METF in this particular malignancy

These results suggest that METF can contribute for the treatment of OS CSCs, as co-adjuvant of DOX or acting alone, directly in CSCs. However, the mechanism of action of this drug is complex; thus, to have a complementary knowledge about METF's action on OS tumors and CSCs a more extensive research is needed.

CHAPTER 6

REFERENCES

---

(1) Demiralp B, Sarkar G, Okuno SH, Yaszemski MJ & Maran A. Osteosarcoma – An Evaluation of Current Diagnosis, Treatment and Chemotherapy. *European Musculoeskeletal Review*, 2011; 6: 18-23

(2) Longhi A, Errani C, De Paolis M, Mercuri M & Bacci G. Primary bone osteosarcoma in the pediatric age: State of art. *Cancer Treatment Reviews*, 2006; 32: 423-436

(3) Osteosarcoma Etiology. *Hindawi Publishing Corporation*, 2011. (0)

(4) Basu-Roy U, Basilico C & Mansukhani A. Perspectives on cancer stem cells in osteosarcoma. *Cancer Letters*, 2012. (0)

(5) Sakamoto A & Iwamoto Y. Current Status and Perspectives Regarding the Treatment of Osteosarcoma: Chemotherapy. *Reviews on Recent Clinical Trials*, 2008; 3: 228-231

(6) Marina N, Gebhardt M, Teot L & Gorlick R. Biology and Therapeutic Advances for Pediatric Osteosarcoma. *The Oncologist*, 2004; 9: 422-441

(7) Wittig JC, Bickels J, Priebat D, Jelinek J, Kellar-Graney K, Shmookler B & Malawer MM. Osteosarcoma: A Multidisciplinary Approach to Diagnosis and Treatment. *American Family Physician*, 2002; 65: 1123-1132

(8) Martin J, Squire JA & Zielenska M. The Genetics of Osteosarcoma. *Hindawi Publishing Corporation*, 2012 (11 pages)

(9) Tang N, Song WX, Luo J, Haydon RC & He TC. Osteosarcoma Development and Stem Cell Differentiation. *Clinical Orthopaedics and Related Research*, 2008; 466: 2114-2130

(10) Molchadsky A, Shats I, Goldfinger N, Pevsner-Fischer M, Olson M, Rinon A, Tzahor E, Lozano G, Zipori D, Sarig R & Rotter V. p53 Plays a Role in Mesenchymal Differentiation Programs, in a Cell Fate Dependent Manner. *PLoS One*, 2008 (15 pages)

(11) Tataria M, Quarto N, Longaker M & Sylvester K. Absence of the p53 tumor supressor gene promotes osteogenesis in mesenchymal stem cells. *Journal of Pediatric Surgery*, 2006; 41: 624-632

(12) Engin F, Bertin T, Ma O, Jiang M, Wang L, Sutton R, Donehower L & Lee B. Notch signaling contributes to the pathogenesis of human osteosarcomas. *Human Molecular Genetics*, 2009; 18: 1464-1470

(13) Gibbs CP, Levings PP & Ghivizzani SC. Evidence for the osteosarcoma stem cell. *Curr Orthop Pract.* 2011; 22: 322-326

(14) Siclari VA & Qin L. Targeting the osteosarcoma cancer stem cell. *Journal of Orthopaedic Surgery and Research*, 2010; 5:78-87

(15) Tolar J, Nauta AJ, Osborn MJ, Mortari A, McElmurry JJ, Bell S, Xia L, Zhou N, Riddle M, Schroeder TM, Westendorf JJ, McIvor R, Hogendoorn P, Szuhai K, Oseth L, Hirsch B, Yant SR, Kay MA, Peister A, Prockop DJ, Fibbe WE & Blazar BR. Sarcoma Derived from Cultured Mesenchymal Stem Cells. *Cancer Stem Cells*, 2007; 25: 371-379

(16) Mosheny AB, Szuhai K, Romeo S, Buddingh EP, Bruijn IB, de Jong D, van Pel M, Cleton-Jansen A & Hogendoom P. Osteosarcoma originates from mesenchymal stem cells in consequence of aneuplodization and genomic loss of Cdkn2. *Journal of Pathology*, 2009; 219: 294-305

(17) Samardziski M, Zafiroski G, Janevska V, Muratovska O, Glamocanin S & Vasilevska-Nikodinovska V. Osteosarcoma: diagnosis and treatment. *Journal of Pediatric Sciences*, 2010; 2: 29

(18) Federman N, Bernthal N, Eilber FC & Tap WD. The Multidisciplinary Management of Osteosarcoma. *Current Treatment Options in Oncology*, 2009; 10:82-93

(19) Martins-Neves S, Lopes A, do Carmo A, Paiva A, Simões P, Abrunhosa A & Gomes C. Therapeutic implications of an enriched cancer stem-like cell population in a human osteosarcoma cell line. *BMC Cancer*, 2012; 12: 139-154

(20) Lewis IJ, Nooji MA, Whelan J, Sydes MR, Grimer R, Hogendoorn P, Memon MA, Weeden S, Uscinska BM, van Glabbeke M, Kirkpatrick A, Hauben EI, Craft AW & Taminiau A. Improvement in Histologic Response But Not Survival in Osteosarcoma Patients Treated With Intensified Chemotherapy: A Randomized Phase III Trial of the European Osteosarcoma Intergroup. *J Natl Cancer Inst*, 2007; 99:112-128

(21) Mintz MB, Sowers R, Brown KM, Hilmer SC, Mazza B, Huvos AG, Meyers PA, LaFleur B, McDonough WS, Henry MM, Ramsey KE, Antonescu CR, Chen W, Healey JH, Daluski A, Berens ME, MacDonald TJ, Gorlick R & Stephan DA. An Expression Signature Classifies Chemotherapy-Resistant Pediatric Osteosarcoma. *Cancer Research*, 2005; 65:1748-1754

(22) Chan H, Grogan TM, Haddad G, DeBoer G & Ling V. P-glycoprotein Expression: Critical Determinant in the Response to Osteosarcoma Chemotherapy. *Journal of the National Cancer Institute*, 1997; 89:1706-1715

(23) Ritter J & Bielack SS. Osteosarcoma. *Annals of Oncology*, 2010; 21:vii320-vii325

(24) Ferrari S, Smeland S, Mercuri M, Bertoni F, Longhi A, Ruggieri P, Alvegard TA, Picci P, Capanna R, Bernini G, Müller C, Tienghi A, Wiebe T, Comandone A, Böhling T, Del Prever AB, Brosjö O, Bacci G & Saeter G. Neoadjuvant Chemotherapy With High-Dose Ifosfamide, High-Dose Methotrexate, Cisplatin and Doxorubicin for Patients With Localized Osteosarcoma of the Extremity: A Joint Study by the Italian and Scandinavian Sarcoma Groups. *Journal of Clinical Oncology*, 2005; 23: 8845-8852

(25) Carrle D & Bielack SS. Current strategies of chemotherapy in osteosarcoma. *International Orthopaedics*, 2006; 30:445-451

(26) Mihm MJ, Yu F, Weinstein DM, Reiser PJ & Bauer JA. Intracellular distribution of peroxynitrite during doxorubicin cardiomyopathy: evidence for selective impairment of myofibrillar creatine kinase. *British Journal of Pharmacology*, 2002; 135: 581-588

(27) Tacar O, Sriamornsk P & Dass CR. Doxorubicin: an update on anticancer molecular action, toxicity and novel drug delivery systems. *Journal of Pharmacy and Pharmacology*, 2012; 65: 157-170

(28) Ugarenko M, Nudelman A, Rephaeli A, Kimura K, Phillips DR & Cutts SM. ABT-737 overcomes Bcl-2 mediated resistance to doxorubicin-DNA adducts. *Biochemical Pharmacology*, 2010; 79: 339-349

(29) Wang D & Lippard SJ. Cellular Processing of Platinum Anticancer Drugs. *Nature Reviews Drug Discovery*, 2005; 4: 307-320

(30) Jamieson ER & Lippard SJ. Structure, recognition and processing of cisplatin-DNA adducts. *Chem. Rev.*, 1999; 99: 2467- 2498

(31) Meyers PA, Schwartz CL, Krailo M, Kleinerman ES, Betcher D, Bernstein ML, Conrad E, Ferguson W, Gebhardt M, Goorin AM, Harris MB, Healey J, Huvos A, Link M, Montebello J, Nadel H, Nieder M, Sato J, Siegal G, Weiner M, Wells R, Wold L, Womer R & Grier H. Osteosarcoma: A Randomized, Prospective Trial of the Addition of Ifosfamide and/or Muramyl Tripeptide to Cisplatin, Doxorubicin, and High-Dose Methotrexate. *Journal of Clinical Oncology*, 2005; 23: 2004- 2011

(32) Kelland L. The resurgence of platinum-based cancer chemotherapy. *Nature Reviews Cancer*, 2007; 7: 573- 584

(33) Jaffe N. High-Dose Methotrexate in Osteosarcoma: Let the Questions Surcease – Time for Final Acceptance. *Journal of Clinical Oncology*, 2008; 26: 4365- 4366

(34) Gonen N & Assaraf YG. Antifolate in cancer therapy: Structure, activity and mechanisms of drug resistance. *Drug Resistance Updates*, 2012; 15: 183-210

(35) Del-Campo LS, Montenegro MF, Saez-Ayala M, Fernandéz-Pérez MP, Cabezas-Herrera J & Rodriguez-Lopez JN. Cellular and molecular mechanisms of Methotrexate resistance in melanoma. *Melanoma- From early detection to treatment,* 2013; 14: 392-409

(36) Gibbs CP, Kukekov VG, Reith JD, Tchigrinova O, Suslov ON, Scott EW, Ghivizzani SC, Ignatova TN & Steindler DA. Stem-like Cells in Bone Sarcomas: Implications for Tumorigenesis. *Neoplasia*, 2005; 7: 967-976

(37) O'Brien CA, Kreso A & Dick JE. Cancer Stem Cells in Solid Tumors: An Overview. *Seminars in Radiation Oncology*, 2009; 19: 71-77

(38) Visvader JE & Lindeman GJ. Cancer Stem Cells: Current Status and Evolving Complexities. *Cell Stem Cell*, 2012; 10: 717- 728

(39) Schackleton M. Normal stem cells and cancer stem cells: similar and different. *Seminars in Cancer Biology*, 2010; 20: 85-92

(40) Jordan CT, Guzman ML & Noble M. Cancer Stem Cells. *The New England Journal of Medicine*, 2006; 355: 1253-1261

(41) Clarke MF, Dick JE, Dirks, PB, Eaves CJ, Jamieson C, Jones DL, Visvader J, Weissman IL & Wahl GM. Cancer Stem Cells – Perspectives on Current Status and Future Directions: AACR Worksop on Cancer Stem Cells. *Cancer Research*, 2006; 66: 9339-9344

(42) Fábián Á, Barok M, Vereb G & Szöllosi. Die Hard: Are Cancer Stem Cells the Bruce Willises of Tumor Biology? *Cytometry Part A*, 2009; 75A: 67-74
(43) Schatton T, Frank NY & Frank MH. Identification and targeting of cancer stem cells. *BioEssays*, 2009; 31: 1038-1049
(44) Li L & Neaves WB. Normal Stem Cells and Cancer Stem Cells: The Niche Matters. *Cancer Research*, 2006; 66: 4553-4557
(45) Bonnet D & Dick JE. Human acute myeloid leukemia is organized as a hierarchy that originates from a primitive hematopoietic cell. *Nature Medicine*, 1997; 3: 730-737
(46) Lapidot T, Sirard C, Vormoor J, Murdoch B, Hoang T, Caceres-Cortes J, Minden M, Paterson B, Caligiuri MA & Dick JE. A cell initiating human acute myeloid leukaemia after transplantation into SCID mice. *Nature*, 1994; 367: 645-648
(47) Al-Hajj M, Wicha MS, Benito-Hernandez A, Morrison SJ & Clarke MF. Prospective identification of tumorigenic breast cancer cells. *Proceedings of the National Academy of Sciences of the United States of America*, 2003; 100: 3983-3988
(48) Eramo A, Lotti F, Sette G, Pilozzi E, Biffoni M, Di Virgilio A, Conticello C, Ruco L, Peschle C & De Maria R. Identification and expansion of the tumorigenic lung cancer stem cell population. *Cell Death and Differentiation*, 2008; 15: 504-514
(49) O'Brien CA, Pollett A, Gallinger S & Dick JE. A human colon cancer cell capable of initiating tumor growth in immunodeficient mice. *Nature*, 2007; 445: 106-110
(50) Li C, Heidt DG, Dalerba P, Burant CF, Zhang L, Adsay V, Wicha M, Clarke MF & Simeone DM. Identification of Pancreatic Cancer Stem Cells. *Cancer Research*, 2007; 67: 1030-1037
(51) Yao Z & Mishra L. Cancer stem cells and hepatocellular carcinoma. *Cancer Biology & Therapy*, 2009; 8: 1691-1698
(52) Singh SK, Hawkins C, Clarke ID, Squire JA, Bayani J, Hide T, Henkelman RM, Cusimano MD & Dirks PB. Identification of human brain tumor initiating cells. *Nature*,2004; 432: 396-401
(53) Visvader JE & Lindeman GJ. Cancer stem cells in solid tumors: accumulating evidence and unresolved questions. *Nature Reviews*, 2008; 8: 755-767
(54) Fulda S. Regulation of apoptosis pathways in cancer stem cells. *Cancer Letters*, 2012.
(55) Tirino V, Desiderio V, d'Aquino R, De Francesco F, Pirozzi G, Galderisi U, Cavaliere C, De Rosa A & Papaccio G. Detection and Characterization of $CD133^+$ Cancer Stem Cells in Human Solid Tumours. *PLoS One*, 2008.
(56) Ribatti D. Cancer stem cells and tumor angiogenesis. *Cancer Letters*, 2012.
(57) Wicha MS, Liu S & Dontu G. Cancer Stem Cells: An Old Idea – A Paradigm Shift. *Cancer Research*, 2006; 66: 1883-1890
(58) Ke J, Wu X, Wu X, He X, Lian L, Zou Y, He X, Wang H, Luo Y, Wang L & Lan P. A subpopulation of $CD24^+$ cells in colon cancer cell lines possess stem cell characteristics. *Neoplasma*, 2012; 59: 282-288

(59) Zhang Y, Wei J, Wang H, Xue X, An Y, Tang D, Yuan Z, Wang F, Wu J, Zhang J & Miao Y. Epithelial mesenchymal transition correlates with $CD24^+$ $CD44^+$ and $CD133^+$ cells in pancreatic cancer. *Oncology reports*, 2012; 27: 1599-1605

(60) Ding XW, Wu JH & Jiang CP. ABCG2: a potential marker of stem cells and novel target in stem cell and cancer therapy. *Life Science*s, 2010; 86: 631-637

(61) Goodell MA, Brose K, Paradis G, Conner AS & Mulligan RC. Isolation and Functional Properties of Murine Hematopoietic Stem Cells that are Replicating In Vivo. *J. Exp. Med.*, 1996; 183: 1797-1806

(62) Wu C & Alman BA. Side population cells in human cancers. *Cancer Letters*,2008; 268: 1-9

(63) Kondo T, Setoguchi T & Taga T. Persistence of a small subpopulation of cancer stem-like cells in the C6 glioma cell line. *Proc. Natl. Acad. Sci.,* 2004; 101: 781-786

(64) Patrawala L, Calhoun T, Schneider-Broussard R, Zhou J, Claypool K & Tang DG. Side Population is enriched in Tumorigenic, Stem-Like Cancer Cells, whereas $ABCG2^+$ and $ABCG2^-$ Cancer Cells are similarly tumorigenic. *Cancer Research*, 2005; 65: 6207-6219

(65) Szotek PP, Pieretti-Vanmarcke R, Masiakos PT, Dinulescu DM, Connolly D, Foster R, Dombkowski D, Preffer F, MacLaughlin DT & Donahoe PK. Ovarian cancer side population defines cells with stem cell-like characteristics and Mullerian Inhibiting Subastance responsiveness. *Proc. Natl. Acad. Sci.*, 2006; 103: 11154-11159

(66) Haraguchi N, Utsunomiya T, Inoue H, Tanaka F, Mimori K, Barnard GF & Mori M. Characterization of a Side Population of Cancer Cells from Human Gastrointestinal System. *Stem Cells*, 2006; 24: 506-513

(67) Oliveira V. Identifying Mechanisms of Resistance to Chemotherapy in Osteosarcoma Tumor Stem Cells [Master Thesis]. Coimbra: Faculdade de Ciências e Tecnologia da Universidade de Coimbra, Curso Engenharia Biomédica, Departamento de Física; 2011

(68) Storms RW, Trujillo AP, Springer JB, Shah L, Colvin OM, Ludeman SM & Smith C. Isolation of primitive human hematopoietic progenitors on the basis of aldehyde dehydrogenase activity. *Proc. Natl. Acad. Sci.*, 1999; 96: 9118-9123

(69) Alison MR, Guppy NJ, Lim S & Nicholson LJ. Finding cancer stem cells: are aldehyde dehydrogenase fit for purpose? *Journal of Pathology*, 2010; 222: 335-344

(70) Ginestier C, Hur MH, Charafe-Jauffret E, Monville F, Dutcher J, Brown M, Jacquemier J, Viens P, Kleer C, Liu S, Schott A, Hayes D, Birnbaum D, Wicha MS & Dontu G. ALDH1 is a marker of normal and malignant human mammary stem cells and a predictor of poor clinical outcome. *Cell Stem Cell*, 2007; 1: 555-567

(71) Ma S, Chan KW, Lee TK, Tang KH, Wo JY, Zheng BJ & Guan XY. Aldehyde dehydrogenase discriminates the CD133 liver cancer stem cell populations. *Molecular Cancer Research*, 2008; 6: 1146-1153

(72) Huang EH, Hynes MJ, Zhang T, Ginestier C, Dontu G, Appelman H, Fields JZ, Wicha MS & Boman BM. Aldehyde dehydrogenase 1 is a marker for normal and malignant human colonic stem cells (SC) and tracks SC overpopulation during colon tumorigenesis. *Cancer Research*, 2009; 69: 3382-3389

(73) Cheung AM, Wan TS, Leung JC, Chan LY, Huang H, Kwong YL, Liang R & Leung YH. Aldehyde dehydrogenase activity in leukemic blasts defines a subgroup of acute myeloid leukemia with adverse prognosis and superior NOD/SCID engrafting potential. *Leukemia*, 2007; 21: 1423-1430

(74) Wang L, Park P, Zhang H, La Marca F & Lin C. Prospective identification of tumorigenic osteosarcoma cancer stem cells in OS99-1 cells based on high aldehyde dehydrogenase activity. *International Journal of Cancer*, 2011; 128: 294-303

(75) Nicolis SK. Cancer stem cells and "stemness" genes in neuro-oncology. *Neurobiology of Disease*, 2007; 25: 217-229

(76) Morrison R, Schleicher SM, Sun Y, Niermann KJ, Kim S, Spratt DE, Chung CH & Lu B. Targeting the mechanisms of resistance to chemotherapy and radiotherapy with the Cancer Stem Cell hypothesis. *Journal of Oncology*, 2011 (13 pages)

(77) Dean M, Fojo T & Bates S. Tumour stem cells and drug resistance. *Nature Reviews*, 2005; 5: 275-284

(78) Rich JN. Cancer stem cells in radiation resistance. *Cancer Research*, 2007; 67: 8980-8984

(79) Bao S, Wu Q, McLendon RE, Hao Y, Shi Q, Hjelmeland AB, Dewhirst MW, Bigner DD & Rich JN. Glioma stem cells promote radioresistance by preferential activation of the DNA damage response. *Nature*, 2006; 444: 756-760

(80) Signore M, Ricci-Vitiani L & De Maria R. Targeting apoptosis pathways in cancer stem cells. *Cancer Letters*, 2013; 332: 374-382

(81) Krajewska M, Moss SF, Krajewski S, Song K, Holt PR & Reed JC. Elevated expression of Bcl-X and reduced Bak in primary colorectal adenocarcinomas. *Cancer Cancer Research*, 1996; 56: 2422-2427

(82) Gonçalves C. Identificação das vias de sinalização anti-apoptóticas em células estaminais cancerígenas de osteossarcoma [Master Thesis]. Coimbra: Faculdade de Ciências e Tecnologia da Universidade de Coimbra, Curso Engenharia Biomédica, Departamento de Física; 2012

(83) Liu G, Yuan X, Zeng Z, Tunici P, Ng H, Abdulkadir IR, Lu L, Irvin D, Black KL & Yu JS. Analysis of gene expression and chemoresistance of $CD133^+$ cancer stem cells in glioblastoma. *Molecular Cancer*, 2006. (12 Pages)

(84) Del Barco S, Vazquez-Martin A, Cufí S, Oliveras-Ferraros C, Bosch-Barrera J, Joven J, Martin-Castillo B & Menendez JA. Metformin: Multi-faceted protection against cancer. *Oncotarget*, 2011; 2: 896-917

(85) Kourelis TV & Siegel RD. Metformin and cancer: new applications for an old drug. *Medical Oncology*, 2012; 29: 1314-1327

(86) Aljada A & Mousa SA. Metformin and neoplasia: Implications and indications. Pharmacology & Therapeutics, 2012; 133: 108-115

(87) Cantrell LA, Zhou C, Mendivil A, Malloy KM, Gehrig PA & Bae-Lump VL. Metformin is a potent inhibitor of endometrial cancer cell proliferation – implications for a novel treatment strategy. *Gynecologic Oncology*, 2010; 116: 92-98

(88) Bao B, Wang Z, Ali S, Ahmad A, Azmi AS, Sarkar SH, Banerjee S, Kong D, Li Y, Thakur S & Sarkar FH. Metformin Inhibits Cell Proliferation, Migration and Invasion by Attenuating CSC Function Mediated by Deregulating mRNAs in Pancreatic Cancer Cells. *Cancer Prevention Research*, 2012; 5: 355-364

(89) Sahra IB, Laurent K, Loubat A, Giorgetti-Peraldi S, Colosetti P, Auberger P, Tanti JF, Marchand-Brustel YL & Bost F. The antidiabetic drug metformin exerts antitumoral effect *in vitro* and *in vivo* through a decrease of cyclin D1 level. *Oncogene*, 2008; 27: 3576-3586

(90) Dowling RJO, Goodwin PJ & Stambolic V. Understanding the benefit of metformin use in cancer treatment. *BMC Medicine*, 2011. (6 Pages)

(91) Sahra IB, Marchand-Brustel YL, Tanti F & Bost F. Metformin in Cancer Therapy: A New Perspective for an Old Antidiabetic Drug? *Molecular Cancer Therapeutics*, 2010; 9: 1092-1099

(92) Dowling JRO, Zakikhani M, Fantus IG, Pollack M & Sonenberg N. Metformin Inhibits Mammalian Target of Rapamycin – Dependent Translation Initiation in Breast Cancer Cells. *Cancer Research*, 2007; 67: 10804-10812

(93) Tomic T, Botton T, Cerezo M, Robert G, Luciano F, Puissant A, Gounon P, Allegra M, Bertolotto C, Bereder J-M, Tartare-Deckert S, Bahadoran P, Auberger P, Ballotti R & Rocchi S. Metformin inhibits melanoma development through autophagy and apoptosis mechanisms. *Cell Death and Disease*, 2011.

(94) Chen G, Xu S, Renko K & Derwahl. Metformin Inhibits Growth of Thyroid Carcinoma Cells, Suppresses Self-Renewal of Derived Cancer Stem Cells, and Potentiates the Effect of Chemotherapeutic Agents. *J Clin Endocrinol Metab*, 2012; 97: 510-520

(95) Memmot RM, Mercado JR, Maier CR, Kawabata S, Fox SD & Dennis PA. Metformin Prevents Tobacco Carcinogenesis- Induced Lung Tumorigenesis. *Cancer Prevention Research*, 2010; 3: 1066-1076

(96) Hundal HS, Ramlal T, Reyes R, Leiter LA & Klip A. Cellular mechanism of metformin action involves glucose transporter translocation from an intracellular pool to the plasma membrane in L6 muscle cells. *Endocrinology*, 1992; 131: 1165-1173

(97) Macheda ML, Rogers S & Best JD. Molecular and Cellular Regulation of Glucose Transporter (GLUT) Proteins in Cancer. *Journal of Cellular Physiology*, 2005; 202: 654-662

(98) Thomas DM, Maher F, Rogers SD & Best JD. Expression and Regulation by Insulin of Glut3 in UMR 106-01, a Clonal Rat Osteosarcoma Cell Line. *Biochemical and Biophysical Research Communications*, 1996; 218: 789-793

(99) Hirsch HA, Iliopoulos D, Tsichlis PN & Struhl K. Metformin Selectively Targets Cancer Stem Cells, and Acts Together with Chemotherapy to Block Tumor Growth and Prolong Remission. *Cancer Research*, 2009; 69: 7507-7511

(100) Takatani T, Minagawa M, Takatani R, Kinoshita K & Kohno Y. AMP-activated protein kinase attenuates Wnt/β-catenin signalling in human osteoblastic Saos-2 cells. *Molecular and Cellular Endocrinology*, 2011; 339: 114-119

(101) Iliopoulos D, Hirsch HA & Struhl K. Metformin Decreases the Dose of Chemotherapy for Prolonging Tumor Remission in Mouse Xenografts Involving Multiple Cancer Cell Types. *Cancer Research*, 2011; 7: 3196-3201

(102) Sylvester PW. Optimization of the tetrazolium dye (MTT) colorimetric assay for cellular growth and viability. *Methods in Molecular Biology*, 2011; 716: 157-168

(103) Bainor A, Chang L, McQuade TJ, Webb B & Gestwicki JE. Bicinchoninic acid (BCA) assay in low volume. *Analytical Biochemistry*, 2011; 410: 310-312

(104) Luo W, Li S, Peng B, Ye Y, Deng X & Yao K. Embryonic Stem Cells Markers Sox2, Oct4 and Nanog Expression and their Correlations with Epithelial-Mesenchymal Transition in Nasopharyngeal Carcinoma. *PLOS One*, 2013; 8: e56324

(105) Levings PP, McGarry SV, Currie TP, Nickerson DM, McClellan S, Ghivizzani SC, Steindler DA & Gibbs CP. Expression of an Exogenous Human Oct-4 Promoter Identifies Tumor-Initiating Cells in Osteosarcoma. *Cancer Res*, 2009; 69: 5648-5655

(106) Moitra K, Lou H & Dean M. Multidrug Efflux Pumps and Cancer Stem Cells: Insights into Multidrug Resistance and Therapeutic Development. *Clin Pharma & Therap*, 2011; 89: 491-502

(107) Gomes CMF, van Paassen H, Romeo S, Welling MM, Feitsma RIJ, Abrunhosa AJ, Botelho MF, Hogendoorn PCW, Pauwels E & Cleton-Jansen AM. Multidrug resistance mediated by ABC transporters in osteosarcoma cell lines: mRNA analysis and functional radiotracer studies. *Nuclear Med and Biol*, 2006; 33: 831-840

(108) Song CW, Lee H, Dings RPM, Williams B, Powers J, Dos Santos T, Choi B-H & Park HJ. Metformin kills and radiosensitizes cancer cells and preferentially kills cancer stem cells. *Scientific reports*, 2012; 362

(109) Motoshima H, Goldstein BJ, Igata M & Araki E. AMPK and cell proliferation – AMPK as a therapeutic target for atherosclerosis and cancer. *The Pysiological Society*, 2006; 574: 63-71

(110) Zakikhani M, Dowling R, Fantus IG, Sonenberg N & Pllack M. Metformin is an AMP Kinase-Dependent Growth Inhibitor for Breast Cells. *Cancer Research*, 2006; 66: 10269-10273

(111) Mitra S, Stemke-Hale K, Mills GB & Claerhout S. Interactions between tumor cells and micro-environment in breast cancer: A new opportunity for targeted therapy. *Cancer Science*, 2012; 103: 400-407

(112) Cairns RA, Harris IS & Mak TW. Regulation of cancer cell metabolism. *Nature Reviews*, 2011; 11: 85-95

(113) Vallabhajosula S. ^{18}F-Labeled Positron Emission Tomographic Radiopharmaceuticals in Oncology: An Overview of Radiochemistry and Mechanisms of Tumor Localization. *Seminars in Nuclear Medicine*, 2007; 37: 400-419

(114) Habibollah P, van den Berg NS, Kuruppu D, Loda M & Mahmood U. Metformin-an Adjunct Antineoplastic Therapy- Divergently Modulates Tumor Metabolism and Proliferation, Interfering with Early Response Prediction by ^{18}F-FDG PET Imaging. *The Journal of Nuclear Medicine*, 2013; 54: 252-258

(115) Würth R, Pattarozzi A, Gatti M, Bajetto A, Corsaro A, Parodi A, Sirito R, Massollo M, Marini C, Zona G, Fenoglio D, Sambuceti G, Filaci G, Daga A, Barbieri F & Florio T. Metformin selectively affects human glioblastoma tumor-initiating cell viability. *Cell Cycle*, 2013; 12: 145-156

(116) Rocha GZ, Dias MM, Ropelle ER, Osório-Costa F, Rossato FA, Vercesi AE, Saad MJA & Carvalheira JBC. Metformin Amplifies Chemotherapy-Induced AMPK Activation and Antitumoral Growth. *Clin Cancer Res*, 2011; 17: 3993-4005